

## **Image-based biological heart age estimation reveals differential aging patterns across cardiac chambers**

Ahmed M Salih (PhD)<sup>1</sup>, Esmeralda Ruiz Pujadas (PhD)<sup>2</sup>, Víctor M. Campello (MSc)<sup>2</sup>, Celeste McCracken (MSc)<sup>3</sup>, Nicholas C Harvey (PhD)<sup>4,5</sup>, Stefan Neubauer (MD)<sup>3</sup>, Karim Lekadir (PhD)<sup>2</sup>, Thomas E Nichols (PhD)<sup>6</sup>, Steffen E. Petersen (DPHIL)\*<sup>1,7,8,9</sup>, Zahra Raisi-Estabragh (PhD)\*<sup>1,7</sup>

<sup>1</sup>William Harvey Research Institute, NIHR Barts Biomedical Research Centre, Queen Mary University of London, Charterhouse Square, London, EC1M 6BQ, UK

<sup>2</sup>Departament de Matemàtiques i Informàtica, Universitat de Barcelona, Artificial Intelligence in Medicine Lab (BCN-AIM), Barcelona, Spain

<sup>3</sup>Division of Cardiovascular Medicine, Radcliffe Department of Medicine, University of Oxford, National Institute for Health Research Oxford Biomedical Research Centre, Oxford University Hospitals NHS Foundation Trust, Oxford, OX3 9DU, UK

<sup>4</sup>MRC Lifecourse Epidemiology Centre, University of Southampton, Southampton, UK

<sup>5</sup>NIHR Southampton Biomedical Research Centre, University of Southampton and University Hospital Southampton NHS Foundation Trust, Southampton, UK

<sup>6</sup>Wellcome Centre for Integrative Neuroimaging, FMRIB, Nuffield Department of Clinical Neurosciences, University of Oxford, Oxford, United Kingdom, Big Data Institute, Li Ka Shing Centre for Health Information and Discovery, Nuffield Department of Population Health, University of Oxford, Oxford, United Kingdom

<sup>7</sup>Barts Heart Centre, St Bartholomew's Hospital, Barts Health NHS Trust, West Smithfield, London, EC1A 7BE, UK

<sup>8</sup>Health Data Research UK, London, UK

<sup>9</sup>Alan Turing Institute, London, UK

\*SEP and ZRE are joint senior authors.

**Corresponding author:** Dr. Ahmed Mahdee Abdo Salih; William Harvey Research Institute, Queen Mary University of London, Charterhouse Square, London, EC1M 6BQ, UK; E-mail: [a.salih@qmul.ac.uk](mailto:a.salih@qmul.ac.uk).

**Running Title:** Heart age estimation in cardiac chambers

## **Competing of interests**

SEP provides consultancy to Cardiovascular Imaging Inc, Calgary, Alberta, Canada. TEN provides consultancy to Perspectum, Oxford, United Kingdom. The remaining authors have nothing to disclose.

## **Funding**

AS was supported by a British Heart Foundation project grant (PG/21/10619). ZR-E recognizes the National Institute for Health Research (NIHR) Integrated Academic Training programme which supports her Academic Clinical Lectureship post and was also supported by British Heart Foundation Clinical Research Training Fellowship No. FS/17/81/33318. SEP acknowledges support from the NIHR Biomedical Research Centre at Barts. SEP has received funding from the European Union's Horizon 2020 research and innovation programme under grant agreement No 825903 (euCanSHare project). SEP acknowledges support from the "SmartHeart" EPSRC programme grant ([www.nihr.ac.uk](http://www.nihr.ac.uk); EP/P001009/1). SEP and SN acknowledge the British Heart Foundation (BHF) for funding the manual image analysis underpinning the creation of a cardiovascular magnetic resonance imaging reference standard for the UK Biobank imaging resource in 5000 scans ([www.bhf.org.uk](http://www.bhf.org.uk); PG/14/89/31194). SN and CM are supported by the Oxford NIHR Biomedical Research Centre (IS-BRC-1215-20008) and the Oxford BHF Centre of Research Excellence. This project was enabled through access to the Medical Research Council (MRC) eMedLab Medical Bioinformatics infrastructure ([www.mrc.ac.uk](http://www.mrc.ac.uk); MR/L016311/1). NCH acknowledges support from MRC (MC\_PC\_21003; MC\_PC\_21001) and NIHR Southampton Biomedical Research Centre. This work was supported by Health Data Research UK, an initiative funded by UK Research and Innovation, Department of Health and Social Care (England) and the devolved administrations, and leading medical research charities. The funders provided support in the form of salaries for authors as detailed above but did not have any additional role in the study design, data collection and analysis, decision to publish, or preparation of the manuscript.

### **Authors contribution**

AS and ZRE conceptualised the work and wrote the manuscript. ERP and VMCR led on extraction and preparation of the radiomics features. AS led on all other analysis steps and prepared all figures and tables. TEN provided expert critical review, and guidance on methods and interpretation of the results. CM supported the analysis. ZRE and SEP provided overall supervision. NCH, SN, and KL provided critical review of the work. All authors read and approved the final manuscript.

### **Acknowledgements**

This study was conducted using the UK Biobank resource under access application 2964. We would like to thank all the UK Biobank participants, staff involved with planning, collection, and analysis, including core lab analysis of the CMR imaging data.

## ABSTRACT

**Background:** Biological heart age estimation can provide insights into cardiac aging.

However, existing studies do not consider differential aging across cardiac regions.

**Purpose:** To estimate biological age of the left ventricle (LV), right ventricle (RV), myocardium, left atrium, and right atrium using magnetic resonance imaging radiomics phenotypes and to investigate determinants of aging by cardiac region.

**Study type:** Cross-sectional.

**Population:** 18,117 healthy UK Biobank participants including 8,338 men (mean age=64.2±7.5) and 9,779 women (mean age=63.0±7.4).

**Field Strength/Sequence:** 1.5 T/balanced steady-state free precession.

**Assessment:** An automated algorithm was used to segment the five cardiac regions, from which radiomic features were extracted. Bayesian ridge regression was used to estimate biological age of each cardiac region with radiomics features as predictors and chronological age as the output. The "age gap" was the difference between biological and chronological age. Linear regression was used to calculate associations of age gap from each cardiac region with socio-economic, lifestyle, body composition, blood pressure and arterial stiffness, blood biomarkers, mental well-being, multi-organ health, and sex hormone exposures (n=49).

**Statistical Test:** Multiple testing correction with false discovery method (threshold=5%).

**Results:** The largest model error was with RV and the smallest with LV age (mean absolute error in men: 5.26 vs 4.96 years). There were 172 statistically significant age gap associations. Greater visceral adiposity was the strongest correlate of larger age gaps, e.g., myocardial age gap in women (Beta=0.85,  $p=1.69 \times 10^{-26}$ ). Poor mental health associated with large age gaps, e.g., "disinterested" episodes and myocardial age gap in men (Beta=0.25,

p=0.001), as did a history of dental problems (e.g., LV in men Beta=0.19, p=0.02). Higher bone mineral density was the strongest associate of smaller age gaps, e.g., myocardial age gap in men (Beta=-1.52, p=7.44x10<sup>-6</sup>).

**Data Conclusion:** This work demonstrates image-based heart age estimation as a novel method for understanding cardiac aging.

**Key words:** aging, cardiac imaging; cardiac health; radiomics.

## INTRODUCTION

Epidemiologic trends indicate aging global populations and increasing burden from diseases of older age(1). Cardiovascular diseases (CVDs) are the most common cause of disability and premature death worldwide and occur more commonly in older individuals(2). Optimizing healthy cardiac aging is a global public health priority(3).

Cardiac imaging may capture distinct age-related cardiac alterations. Magnetic resonance imaging (MRI) is the reference modality for cardiac chamber quantification and can provide evaluation of myocardial tissue character(4).

MRI derived phenotypes (IDPs) permit non-invasive characterization of cardiovascular health and detection of preclinical organ-level remodeling (5). Alteration of MRI phenotypes reflects exposure to specific cardiovascular stressors, which may differentially impact individual cardiac chambers. For instance, chronic pulmonary disorders are known to preferentially impact right atrial and right ventricular phenotypes(6); whilst hypertension related remodeling primarily affects the left heart(7). Thus, the exposure profile of an individual can determine the pattern of aging across different heart structures. The recognition of such remodeling patterns is important, as they have different clinical and

prognostic consequences. Furthermore, the pattern of remodeling associated with an exposure can provide insight into the mechanisms through which it alters cardiovascular health.

In previous reports, researchers have used deep learning methods applied to cardiovascular imaging to develop estimates of heart age(8,9). These studies present novel approaches to evaluating heart age based on its image appearance. However, given the “black box” nature of these methods, the interpretability of the developed models is limited. Importantly, it is not possible to highlight the precise impact of an exposure on specific cardiac structures. This severely limits biological and clinical inferences from such models.

MRI radiomics analysis permits extraction of many quantitative measures of cardiac shape and myocardial character using voxel-level data(5). The large number of features generated lends itself ideally to machine learning methods. A key advantage of MRI radiomics features over black box methods is the potential to produce interpretable models.

We hypothesized that heart age of individual cardiac structures may be modeled using radiomics features extracted from related regions i.e., it may be possible to describe, in a quantitative and interpretable manner, differential aging patterns across cardiac chambers. This information could in turn be used to evaluate patterns of aging across different cardiovascular structures ascribed to specific exposures.

The aim of this study was to use MRI radiomics features to estimate biological age of the left and right ventricles (LV, RV) and atria (LA, RA), and the LV myocardium. A further aim was to investigate the association of selected exposures on aging across these structures, separately in men and women.

## **MATERIALS AND METHODS**

### ***Data Source and Population Characteristics***

The UK Biobank comprises detailed characterization of approximately 500,000 individuals from across the UK. The participants were aged 40-69 at recruitment (2006 to 2010).

Baseline assessment was conducted according to a published research protocol(10), gathering information on demographic, lifestyle and environment factors, cognitive tests, and blood sampling. The UK Biobank Imaging Study was launched in 2015 and is ongoing, aiming to perform multiorgan imaging for a 20% (n=100,000) subset of the original participants. In this study, we included 29,144 participants for whom MRI data were available. We excluded 11,027 participants with history of CVD at time of imaging (*Supplementary Table 1*). The analysis sample included 8,338 men and 9,779 women. The average age was 64.2 ( $\pm 7.5$ ) years for men and 63.0 ( $\pm 7.4$ ) years for women.

### ***Image Acquisition***

Imaging was performed in dedicated UK Biobank centers using uniform staff training, equipment, and pre-defined acquisition protocols(11). MRI scans were performed using 1.5 Tesla scanners (MAGNETOM Aera, Syngo Platform VD13A, Siemens Healthcare, Erlangen, Germany). Cardiac structure and function were assessed using standard long axis slices (vertical long axis, horizontal long axis and left ventricular outflow tract) and a short axis stack covering the ventricles from base to apex. All cine images were acquired with a balanced steady state free precession sequence. The imaging protocol parameters were set to as slice thickness (6.0), matrix size (208 x 187), voxel size (1.8 x 1.8 x 6.0), TR (ms) (2.7), TE(ms) (1.16) and acquired temporal resolution (ms) (32.64). Further details of pulse sequence parameters have been previously published(11).

### ***Image Segmentation* Image segmentation**

We computed radiomics features from the voxels identified by the atrial contours from long axis and the RV, LV, and LV myocardium from short axis images, in end-systole and end-diastole. Automated segmentation of the ventricular and myocardial regions was performed using a previously developed pipeline, trained on a large expert annotated manual segmentation dataset. End-diastolic was considered as the first phase of the acquisition. Experts determined the end-systolic phase visually by which the LV intra-cavity blood pool is in its smallest size at the mid-ventricular level (12).

To define the atrial contours from the long axis images, an automatic segmentation model based on a traditional U-Net architecture was implemented. Ground truth manually annotated datasets (n= 764) were used for model fitting(12). Data augmentation techniques were used to introduce more variability in the overall structure and appearance of images and to improve the generalizability of the model. These included small rotations of the image, random bias field perturbations, random contrast adjustments and random intensity histogram shifting. The model was trained for 100 epochs with a batch size of 16 on 256x256 images using the Adam optimizer with a learning rate of 0.0001 and 0.9 and 0.999 first and second moments, respectively. Binary cross entropy was used as loss function. The resulting model was used to generate automatic delineations for the rest of the studies considered in this work. Two post-processing steps were used to ensure smooth contours: an algorithm to fill potential holes in the final mask and a selection of the largest connected component predicted for each region of interest (ROI). A fully automated quality-controlled image analysis pipeline, previously developed and validated in a large subset of the UK Biobank(13)(12), was applied to short axis images to define the LV, RV, and myocardial contours.



For each study, the RV, LV, and myocardial contours were automatically defined and exported in a single xml file. We developed an in-house software in Python (version 3.7.9) to convert the contours into binary masks, which we have made publicly available(14). This software builds a polygon from the contour points in the coordinate space to form the mask, given the xml file and the corresponding MR DICOM images. The area bounded by the contour in every slice was filled with ones using the fillpoly function from the OpenCV(15) library, resulting in the binary ROI. This process was repeated for all delineated contours. For the atrial contours, the deep learning method was designed to automatically return a binary mask without the need for any intermediate steps.

### ***Feature Extraction***

The open-source PyRadiomics platform (version 2.2.0.) was used to extract Radiomics features given the contours and the corresponding images. For intensity-based and texture features, brightness harmonization was achieved by histogram standardization, and gray values were discretized with a bin width of 25 (units). For each frame, we computed 13 shape, 18 first-order, and 75 texture features. In the long axis, one 3D shape feature, “flatness”, was discarded in outlier removal checks. The texture features were extracted using five different matrices: gray-level co-occurrence matrix (24 features), gray-level run-length matrix (16 features), gray-level size-zone matrix (16 features), neighboring gray tone difference matrix (5 features), and gray-level dependence matrix (14 features). In all, we computed a total of 210 radiomics features for each ROI (shape n=24, first-order n=36, texture n=150). The full list of the radiomic features extracted is displayed in ***Supplementary Table 2***. Further background information to radiomics, can be found in dedicated review articles(5,16–18).

### ***Feature Selection***

All the following steps were implemented using Python 3.8.10 and Scikit-learn 1.0.2. A total of 1,050 radiomics features were available (210 from each of 5 ROIs (LV, RV, LA, RA, myocardium)). We built individual models for each ROI, separately for men and women, resulting in a total of 10 models. Model development methods were uniform across all 10 models. First, we applied recursive feature elimination with cross-validation (RFECV) to choose the optimal number of features (among the 210 per ROI) using Bayesian ridge regression(19) as the model (10-fold), and with chronological age set as the dependent variable. Thereafter, we applied Cook's Distance(20) method to detect and remove any outliers. A data point was considered an outlier by Cook's Distance if its value was larger than 3 times the mean of all the data points (*Supplementary Table 3*).

### ***Model Building***

Figure 1 explains the overall of the study and modeling. Height and weight were considered as confounds and regressed out from the features using a linear regression model where the confounds are the independent variables and each feature is the dependent variable.

Thereafter, the features were normalized to have zero mean and unit variance. Bayesian ridge regression was used to estimate the age of each ROI. The "age gap" values were calculated by subtracting the actual age from the predicted age for each cardiac structure (or ROI). We examined the association of age gap metrics with lifestyle and health exposures.

### ***Explainability***

To aid interpretability of our models, we identified the most informative features driving the model output using the SHapley Additive exPlanations (SHAP) method. SHAP calculates a value for each radiomics feature representing the contribution of that feature to the model output. The output of SHAP is a list of the most informative features in the model in

descending order. The list is based on the SHAP value for each feature in the model which quantifies the impact (magnitude, direction) of the feature on the model output.

### ***Associations of Age Gap with Selected Exposures***

We considered associations between age gap from each structural region and a selection of key exposures selected based on biological knowledge of their associations with cardiovascular health. We considered 49 exposures (***Supplementary table 4***), including socio-economic factors (n=5), lifestyle factors (n=6), obesity and body composition metrics (n=9), blood pressure and arterial stiffness (n=4), blood biomarkers (n=7), mental well-being (n=6), multi-organ health indicators (n=10) and Sex hormones (n=2). The following quality control steps were performed on the exposures before investigating the association with age gap. Levels within categorical variables were re-ordered to align higher scores with healthier exposure levels (applies to educational level, health satisfaction, financial satisfaction). Blood pressure and resting heart rate were limited to biologically plausible ranges: systolic blood pressure: >60mmHg and <200mmHg; diastolic blood pressure: >40 mmHg and <120mmHg), resting heart rate: >40bpm and <140bpm. Blood biochemistry parameters were restricted to values within the manufacturer's analytical range(21).

### ***Statistical Analysis***

Model performance was assessed using Mean Absolute Error (MAE) and Prediction Coefficient of Determination ( $R^2$ ). MAE is the difference between the predicted value (estimated heart age) and the actual value (actual age). Prediction  $R^2$  measures how much of the variation in the outcome (predicted heart age) is explained by the input data (radiomics features) and is calculated as: Prediction  $R^2 = 1 - \text{Prediction mean squared error} / \text{total sum of squares}$ . We applied a regression to the mean correction to remove dependency of heart age gap (delta) on age(22).

Linear regression was used to examine associations of heart age gap from each ROI with each exposure. Models were adjusted for height, weight, and age. We report beta coefficients and 95% confidence intervals (CI) relating to the age gap value associated with each exposure – which indicates difference in cardiac age (for each anatomic region) for each unit increase in the exposure. A positive beta value indicates direction of association towards a more positive age gap – i.e., greater cardiac age than actual age (likely adverse exposure). We corrected for multiple testing using the false discovery rate method (threshold  $p < 0.05$ ).

## **RESULTS**

### ***Baseline characteristics***

Compared to women, men had poorer cardiometabolic profile, with greater obesity, poorer glycemic control, and higher blood pressure and arterial stiffness. Women had, on average, greater levels of deprivation, lower educational level, and lived in lower income households. Women also scored higher on all indicators of poorer mental wellbeing. More details of baseline population characteristics are explained in table 1.

### ***Model Performance***

We present model performance metrics in **Table 2** as the average MAE and predicted  $R^2$  across all folds (from our 10-folds cross validation) for each ROI in men and women, before application of the regression to the mean correction. Across all cardiac regions, age estimation models had greater error in men (higher MAE, lower  $R^2$ ) than women. For both men and women, the greatest discrepancy between model estimated age and chronological age was observed for the RV followed by the myocardium, as indicated by greatest error in these models (higher MAE, lower  $R^2$ ). In comparison, LV cavity age estimation models had the best performance metrics (lower MAE, higher  $R^2$ ).

### ***Left Atrium***

Geometric alterations of the LA (radiomics shape features) were informative age-related metrics (major and minor axis length, 2D diameter row and column) in both women and men, all indicating that greater LA age was linked to smaller chamber size (**Figure 2**). In women, we additionally observed that smaller surface area, mesh volume, and voxel volume were all linked to greater LA age. SI-based features had a more minor role in these models, however overall, they indicated that greater LA age gap was linked to smoother less coarse texture in the LA blood pool (e.g., lower autocorrelation) in both men and women (**Figure 2**).

### ***Left Ventricle***

In both men and women, radiomics phenotypes indicating smaller and less spherical LV shape were amongst the most informative individual model features according to SHAP values (**Figure 2**). Signal intensity (SI)-based features also contributed importantly to models for men and women including features indicating greater skewness and variance in men. In women, features indicating greater autocorrelation of LV cavity pixel intensities (greater coarseness) and high gray level emphasis were informative. Another notable result is that the range of SHAP values in female cohorts was bigger than in the male cohort indicating greater impact of these features in the age model for women.

### ***LV Myocardium***

In men, shape features were most informative to LV myocardial age estimation, while for women myocardial SI-based features were more prominent (**Figure 2**). In men, greater myocardial age was linked to smaller surface area, larger voxel volume, and smaller minor and major axis lengths. In women, myocardial age was indicated by features representing a dimmer and more homogenous pattern of myocardial SI. For instance, in women, greater myocardial age was linked to lower mean gray level intensity level (lower “joint average”),

higher proportion of low SI pixel pairs in relation to high SI pairs (lower “sum average”), and less variation in intensity levels (lower “skewness”, higher “low run gray level emphasis”). The intensity variations related to myocardial age in men were in a similar direction to those in women but were less extensive and less informative to the overall model (**Figure 2**).

### ***Right Atrium***

The list of most informative predictors produced by SHAP shows that the most informative features for the RA age model were dominated by texture features in both men and women (**Figure 3**). In men, greater RA age was linked to smaller RA size (lower major axis length in end-diastole and end-systole), and greater homogeneity in RA (lower: “dependence non-uniformity”, “cluster prominence”, “difference average”). In women, greater RA age was linked to larger RA size (higher “maximum 2D diameter column”) and higher heterogeneity of RA blood pool pixel intensities (higher: “gray level non-uniformity”, “contrast”, “sum squares”).

### ***Right Ventricle***

In women, greater RV age was linked to smaller chamber size (lower “mesh volume”, increasing R “maximum 2D diameter row”), less spherical RV shape (lower “sphericity”), and greater surface area of the cavity (higher “surface area”). In men, greater RV age was linked to larger “minor axis length”, lower “maximum 2D diameter”, and lower “major axis length” (**Figure 3**). In women, increasing RV age was also linked to greater “autocorrelation”, indicating coarser pattern of blood pool SIs. In men, the informative SI-based features indicated a less complex pattern of SIs (lower “complexity”) and greater variation in SI levels (“gray level variance”).

### ***Exposure Associations with Heart Age Gap***

A total of 172 associations showed significant relationships with heart age gap in both women and men across the five ROIs. The largest number of associations was observed with the LV myocardium (n=52) age gap with 52 significant associations divided into 27 in men and 25 in women. The LV (n=44) and RV (n=20) had the second and third highest number of significant associations with the tested exposures. On the other hand, LA had fewer associations with the tested exposures with only 15 significant associations, 8 in women and 7 in men (***Table 3***).

In terms of the number of significant associations in each of the exposure categories, obesity and body composition metrics were dominant (51 significant associations), showing consistent associations between greater adiposity and with larger heart age gap across all cardiac structures (***Table 4***). Granular results of all exposure associations are available in ***Supplementary table 4*** and are summarized in ***Figure 4***.

Amongst the obesity measures considered, the strongest (largest magnitude) association was observed with visceral adiposity derived from abdominal MRI scans. Greater waist circumference was positively associated with heart age gap in both men and women. The relationships with obesity, across all the metrics, appeared stronger in women than in men. Higher high-density lipoprotein (HDL) cholesterol was linked to greater heart age gap across the LV, RV, and myocardium, having stronger association in women than in men. The magnitude of this association appeared greatest with the LV myocardium age gap (higher HDL, smaller heart age gap). Higher levels of low-density lipoprotein (LDL) cholesterol and triglyceride were linked to higher age gaps, although the magnitude of these associations was smaller than with HDL cholesterol.

Higher diastolic blood pressure, faster resting heart rate, and greater arterial stiffness were all significant positive associates of heart age gap, although the magnitude of these associations was small.

Indicators of better multi-organ health, such as higher hand grip strength (right, left), forced vital capacity, and heel bone mineral density were linked to smaller heart age gaps. Notably, for both men and women, better bone health as indicated by greater heel bone mineral density, showed the largest magnitude association with smaller heart age gap of all exposures considered.

In our sample, socio-economic and lifestyle factors showed few significant associations with heart age gap. The number of vehicles in household, education level, and the Townsend score (measure of deprivation) did not show any significant ( $p$ -value  $> 0.05$ ) association with heart age gap. In terms of daily lifestyle factors, greater physical activity levels were linked to smaller heart age gap in men (myocardium, LV, RV) and women (LV). Smoking, beef, and pork intake did not show any significant ( $p$ -value  $> 0.05$ ) associations. Greater time spent watching television was associated with greater RV and myocardium heart age gaps in men. Higher testosterone level was observed with larger age LV age gap (greater biological aging) in men (coefficient 0.08,  $p$ -value = 0.03).

## **DISCUSSION**

In this study, we present age estimation models for key cardiac structures developed using cardiac MRI radiomics phenotypes in 18,117 UK Biobank participants free from clinical CVD. We selected this model due to its ability to handle the collinearity among the model predictors(23,24). We considered discrepancy in age estimation from chronological age (heart age gap) as an indicator of greater cardiac aging, demonstrating differential aging



patterns across heart structures and the associations of selected exposures with greater age gap.

Amongst the cardiac regions modelled, the LV age models had the best performance, whilst the RV models had the greatest error. This is in keeping with known greater anatomic complexity and irregularity of the RV (25) compared to the LV, which is reflected in greater heterogeneity of RV phenotypes and greater error in our age models. Model performance showed greater error in men than women across all regions modelled, possibly indicating greater variation of IDPs in men.

The error in biological age estimation model comprises model error and biological age gap. In our study, we modelled biological age for the four cardiac chambers and the LV myocardium, observing different magnitude of error across these cardiac sites. This may reflect more advanced aging in cardiac regions with larger model error. For instance, the RV biological age estimation model had the largest MAE, which may indicate greater susceptibility of the RV to age-related remodelling and greater biological aging in this chamber compared to other cardiac regions. The second largest error was in the model for myocardial biological age, which may highlight that the myocardium is also a site where age-related alterations are prominent. In comparison, the LV had the smallest MAE of all chambers modelled, perhaps indicating that morphological age-related alterations of the LV are less pronounced or occur at more advanced stages compared to other chambers. Alternatively, it is possible that the larger model error reflects “actual” error, that is poorer model performance in age estimation for the RV and myocardium, and better performance in age estimation for the LV. While it is not possible to definitively disentangle these two components of error, it is likely that they both contribute somewhat to the magnitude of MAE in our models (26).

In evaluating the most informative features, overall, we observed importance of both shape and signal intensity based radiomics features. Several features appeared informative across all ROI models. For instance, the major and minor axis length and surface area in the shape feature group were among the top informative predictors in the most regions and in both male and female cohorts. In addition, auto-correlation from the texture feature group frequently appeared among the most informative features. The presence of these features in all examined regions in both male and female cohorts highlights their potential value as predictors in cardiac phenotype studies. The impact of the features on the model outcome was different from one ROI to another based on the SHAP value. For example, the range of the SHAP values for the features in the RA (female cohort) was smaller than in other regions. On the other hand, the impact of the features on the outcome was the largest when modelling LV age in women. Furthermore, the impact of the features on the outcome between male and female was different in some regions including LA, LV, and RV.

We evaluated associations of exposures with heart age gap metrics. The myocardial age gap had the largest number of significant associations, indicating that age-related changes of the myocardium are importantly influenced by a wide range of different exposures. Obesity was a prominent associate of greater age gap across all cardiac structures, as represented by image-derived measures of obesity, body size measures, and blood lipids. These associations were stronger in women than men. The myocardium and LV age gaps showed a greater number of significant associations with the exposures examined than the other regions, while LA and RA had fewer associations. In both men and women, significant associations between greater age gap of the LV, RV and myocardium were observed across a range of exposures including higher visceral adipose tissue volume, pulse rate, total trunk fat volume, abdominal subcutaneous adipose tissue volume, trunk fat mass and whole body fat

mass. The most significant associations with myocardium and LV age gap were exposures from multi-organs indicators and obesity and body composition metrics.

MRI is unique as a modality in its ability to non-invasively characterize myocardial tissue. Previous work using MRI radiomics has demonstrated the value of radiomics signal-intensity based features extracted from the LV myocardium in discriminating disease states (27–29). The use of MRI radiomics is currently limited to research settings and further research is required before implementation in clinical settings. Other methods for myocardial tissue characterization include non-parametric mapping techniques and contrast-enhanced image acquisitions. Late gadolinium enhancement (LGE) techniques are most established, and their clinical utility has been demonstrated in multiple previous studies in the setting of both ischemic and non-ischemic cardiomyopathies(30,31). The use of LGE acquisitions is accordingly widely adopted in clinical settings. Greater scan time (approx. 15 mins) as well as a small risk associated with intravenous gadolinium administration are drawbacks of this technique (32). Non-parametric mapping methods (T1, T2, T2\*) have shown utility in disease discrimination and outcome prediction in multiple settings(33). These are non-contrast methods but do require dedicated specialist acquisitions. Although these methods are implemented in clinical practice, there are many outstanding technical issues, in particular regarding standardization of the techniques, that currently limited widespread generalizability (34). Furthermore, the role of these metrics in the setting of a healthy population is not yet definitively established.

Previous studies have examined associations of myocardial native T1 and T2 with increasing age. A large population study in the UK Biobank found increasing age-related increase in myocardial native T1 in men and a decreasing trend in women (35). A smaller study of the Multi-Ethnic Study of Atherosclerosis) cohort reports positive association of native T1 with increasing age in men, but no significant age trend in women (35). The age-

dependency of T2 is less consistent, with some researchers reporting no relationship between T2 and age (36), whilst others report a decreasing trend (37). In our analysis, we used shape and signal-intensity based radiomics features extracted from bSSFPF short axis cine images. The association of these features with T1 and T2 extracted from mapping sequences is not known.

A key advantage of radiomics analysis is that it can be applied to existing standard of care contrast-free images, presenting a potentially highly efficient method for tissue characterization. Our findings suggest that myocardial signal intensity radiomics features may provide important information about myocardial aging in population cohorts. Our work encourages further research in this area to determine the clinical utility of this technique.

Of all the exposures considered, measures of obesity and serum lipids showed the most prominent associations with greater heart age gap across all the structures considered, appearing more important in women than men. Obesity is a global public health priority and its associations with adverse cardiovascular health are widely reported(38). Furthermore, others have reported phenotypic alterations of the LV in association with greater obesity (39) The association of obesity exposures with greater heart age gap support the validity of our age estimation models. Furthermore, our study has described the associations of obesity with cardiac aging (as defined by age-related phenotypic alterations) across all key cardiac chambers. Our observations highlight the importance of tackling obesity for alleviation of the global burden of cardiovascular disease. The strongest associations were with abdominal MRI measures of obesity (visceral adipose tissue volume, abdominal subcutaneous adipose tissue volume, and total trunk fat volume). Notably, of the anthropometric measures of obesity, waist circumference showed stronger associations to larger heart age gap than body mass index, indicating the value of this metric in assessment of obesity-related cardiovascular risk. Furthermore, although the baseline levels of obesity were greater for men, their

associations with greater heart aging were stronger in women than men. This may indicate differential magnitude of the cardiovascular impact of obesity in women, and warrants further dedicated study. Higher blood pressure, resting heart rate, and arterial stiffness were associated with significantly larger heart age gap across most cardiac regions. This observation highlights the utility of these established vascular health indicators as indices for monitoring heart aging.

### ***Limitations***

The UK Biobank provided access to a large bank of uniformly acquired cardiac MR scans, which was essential for development of our models. The detailed characterization of participants permitted reliable ascertainment of health status using UK Biobank assessments and linked health records. However, given that our models were developed on a healthy population-based cohort, further study is required to determine if the observations made translate to a clinical cohort. Second, our models performed well within this dataset of homogeneously acquired scans. However, cardiac MR radiomics features are susceptible to variation in pulse sequence parameters, scanner vendor, and case mix(40). Thus, these models may not perform in the same way in external cohorts. Third, our findings suggest that the age gap metrics extracted from our models may be useful as imaging biomarkers of cardiovascular health. However, direct comparison of our work with existing publications is challenging. Fourth, in this study, we used a simple model to estimate heart age to establish a benchmark for more complex methods with potentially better performance, as heart age modelling is not well-established as it is for other organs such as brain age estimation. In the latter, there is a well described regression to the mean effect, which we also observed in our analysis. We opted to correct for this with the widely used method proposed by Beheshti et al.(22). A limitation of this approach is false improvement of model performance(26); with this in mind, we report pre-corrected performance metrics in this study. The correction is not

expected to influence exposure associations with heart age gap (delta). Fifth, the clinical interpretation of the radiomics features in the model is not known as they have not been used and examined widely in morbidities and phenotypes to establish connections between the features and clinical outcomes. However, more work in this direction may solve the issues raised above. Further work is required to determine the clinical utility of these metrics. Moreover, we limit our study to participants without clinically diagnosed cardiovascular disease. As we do not have access to clinically evaluate individual patients, we cannot exclude undiagnosed disease in the study sample.

### ***Conclusion***

We demonstrate an interpretable model for biological age estimation across different cardiac structures developed using cardiac MRI radiomics phenotypes. Our findings indicate that discrepancy in image-based age estimates and chronological age (heart age gap) may be a useful indicator of cardiovascular health, and specifically for investigation of cardiovascular aging. A key advantage of the biological age estimation models presented in our study, is that the radiomics features extracted are obtained from routinely acquired standard of care cine MRI images. This means that our models have potential for broad application across research and clinical studies.

Our findings demonstrate obesity as an important correlate of heart aging, highlighting the importance of public health strategies for tackling obesity in ensuring population cardiovascular health. Further work is required to establish the potential wider utility of age gap metrics extracted from our models for risk estimation and outcome prediction.

## **DECLARATIONS**

### **Ethics approval and consent to participate**

This study complies with the Declaration of Helsinki; the work was covered by the ethical approval for UK Biobank studies from the National Health Service (NHS) National Research Ethics Service on 17th June 2011 (Ref 11/NW/0382) and extended on 18 June 2021 (Ref 21/NW/0157) with written informed consent obtained from all participants.

### **CONSENT FOR PUBLICATION**

All the authors are accepted to publish the manuscript.

### **AVAILABILITY OF DATA AND METRIALS**

The dataset supporting the conclusions of this article is available in the UK Biobank repository, under access application 2964, <http://www.ukbiobank.ac.uk/register-apply>.

UK Biobank will make the data (including image acquisition parameters) available to all bona fide researchers for all types of health-related research that is in the public interest, without preferential or exclusive access for any persons. All researchers will be subject to the same application process and approval criteria as specified by UK Biobank.

### **References**

1. World Health Organization (WHO). Global Health and Aging. 2011.
2. Roth GA, Mensah GA, Johnson CO, Addolorato G, Ammirati E, Baddour LM, et al. Global Burden of Cardiovascular Diseases and Risk Factors, 1990–2019. *J Am Coll Cardiol*. 2020 Dec;76:2982–3021.
3. “Ageing well” must be a global priority [Internet]. [cited 2023 Feb 13]. Available from: <https://www.who.int/news/item/06-11-2014--ageing-well-must-be-a-global-priority>
4. Lombardi M, Plein S, Petersen S, Bucciarelli-Ducci C, Buechel EV, Basso C, et al., editors. *The EACVI Textbook of Cardiovascular Magnetic Resonance*. The EACVI Textbook of Cardiovascular Magnetic Resonance. Oxford University Press; 2018.
5. Raisi-Estabragh Z, Izquierdo C, Campello VM, Martin-Isla C, Jaggi A, Harvey NC, et

- al. Cardiac magnetic resonance radiomics: basic principles and clinical perspectives. *Eur Hear J - Cardiovasc Imaging*. 2020 Apr 1;21:349–56.
6. Prins KW, Rose L, Archer SL, Pritzker M, Weir EK, Olson MD, et al. Clinical determinants and prognostic implications of right ventricular dysfunction in pulmonary hypertension caused by chronic lung disease. *J Am Heart Assoc*. 2019 Jan;8:1–15.
  7. Rodrigues JCL, Amadu AM, Dastidar AG, Szantho G V., Lyen SM, Godsave C, et al. Comprehensive characterisation of hypertensive heart disease left ventricular phenotypes. *Heart*. 2016 Oct;102:1671–9.
  8. Abstract 12758: Dissecting Heart Age Using Cardiac Magnetic Resonance Videos, Electrocardiograms, Biobanks, and Deep Learning | *Circulation*. *Circulation*. 2021;
  9. Chang CH, Lin CS, Luo YS, Lee YT, Lin C. Electrocardiogram-Based Heart Age Estimation by a Deep Learning Model Provides More Information on the Incidence of Cardiovascular Disorders. *Front Cardiovasc Med*. 2022 Feb 8;9:1–14.
  10. UK Biobank Coordinating Centre. UK Biobank: Protocol for a large-scale prospective epidemiological resource. Vol. 06, UKBB-PROT-09-06 (Main Phase). 2007. p. 1–112.
  11. Petersen SE, Matthews PM, Francis JM, Robson MD, Zemrak F, Boubertakh R, et al. UK Biobank’s cardiovascular magnetic resonance protocol. *J Cardiovasc Magn Reson*. 2015 Dec;18(1):8.
  12. Petersen SE, Aung N, Sanghvi MM, Zemrak F, Fung K, Paiva JM, et al. Reference ranges for cardiac structure and function using cardiovascular magnetic resonance (CMR) in Caucasians from the UK Biobank population cohort. *J Cardiovasc Magn Reson*. 2017 Feb 3;19:1–19.
  13. Bai W, Sinclair M, Tarroni G, Oktay O, Rajchl M, Vaillant G, et al. Automated cardiovascular magnetic resonance image analysis with fully convolutional networks. *J Cardiovasc Magn Reson*. 2018/09/16. 2018;20(1):65.
  14. GitHub - euCanSHare/dicom2nitfi: Tool for medical image conversion from DICOM to NIFTI format.
  15. OpenCV: OpenCV modules [Internet]. [cited 2023 Feb 13]. Available from: <https://docs.opencv.org/3.4/index.html>
  16. Gillies RJ, Kinahan PE, Hricak H. Radiomics: Images Are More than Pictures, They Are Data. *Radiology*. 2016 Feb;278:563–77.
  17. Lambin P, Leijenaar RTH, Deist TM, Peerlings J, De Jong EEC, van Timmeren J, et al. Radiomics: The bridge between medical imaging and personalized medicine. *Nat Rev Clin Oncol*. 2017 Dec;14:749–62.
  18. Aerts HJWL. The Potential of Radiomic-Based Phenotyping in Precision Medicine. *JAMA Oncol*. 2016 Dec;2:1636–42.
  19. MacKay DJC. Bayesian Interpolation. *Neural Comput*. 1992 May;4:415–47.
  20. Bengfort B, Bilbro R. Yellowbrick: Visualizing the Scikit-Learn Model Selection Process. *J Open Source Softw*. 2019 Mar;4:1075.
  21. Fry D, Almond R, Moffat S, Gordon M, Singh P. UK Biobank Biomarker Project Companion Document to Accompany Serum Biomarker Data. 2019. p. 1–16.



22. Beheshti I, Nugent S, Potvin O, Duchesne S. Bias-adjustment in neuroimaging-based brain age frameworks: A robust scheme. *NeuroImage Clin.* 2019;24:1–6.
23. Assaf AG, Tsionas M, Tasiopoulos A. Diagnosing and correcting the effects of multicollinearity: Bayesian implications of ridge regression. *Tour Manag.* 2019 Apr;71:1–8.
24. Efendi A, Effrihan. A simulation study on Bayesian Ridge regression models for several collinearity levels. In: *AIP Conference Proceedings*. AIP Publishing LLC AIP Publishing; 2017. p. 1–6.
25. Ammari A, Mahmoudi R, Hmida B, Saouli R, Bedoui MH. A review of approaches investigated for right ventricular segmentation using short-axis cardiac MRI. *IET Image Process.* 2021 Jul 1;15:1845–68.
26. Butler ER, Chen A, Ramadan R, Le TT, Ruparel K, Moore TM, et al. Pitfalls in brain age analyses. *Hum Brain Mapp.* 2021;42:4092–101.
27. Neisius U, El-Rewaify H, Nakamori S, Rodriguez J, Manning WJ, Nezafat R. Radiomic Analysis of Myocardial Native T1 Imaging Discriminates Between Hypertensive Heart Disease and Hypertrophic Cardiomyopathy. *JACC Cardiovasc Imaging.* 2019 Oct;12:1946–54.
28. Cetin I, Petersen SE, Napel S, Camara O, Ballester MAG, Lekadir K. A Radiomics Approach to Analyze Cardiac Alterations in Hypertension. In: *2019 IEEE 16th International Symposium on Biomedical Imaging (ISBI 2019)*. IEEE; 2019. p. 640–3.
29. Baessler B, Mannil M, Oebel S, Maintz D, Alkadhi H, Manka R. Subacute and Chronic Left Ventricular Myocardial Scar: Accuracy of Texture Analysis on Nonenhanced Cine MR Images. *Radiology.* 2018 Jan;286:103–12.
30. Alba AC, Gaztañaga J, Foroutan F, Thavendiranathan P, Merlo M, Alonso-Rodriguez D, et al. Prognostic Value of Late Gadolinium Enhancement for the Prediction of Cardiovascular Outcomes in Dilated Cardiomyopathy: An International, Multi-Institutional Study of the MINICOR Group. *Circ Cardiovasc Imaging.* 2020;13:1–12.
31. Green JJ, Berger JS, Kramer CM, Salerno M. Prognostic Value of Late Gadolinium Enhancement in Clinical Outcomes for Hypertrophic Cardiomyopathy. *JACC Cardiovasc Imaging.* 2012 Apr;5:370–7.
32. Ehara S, Matsumoto K, Kitada R, Nishimura S, Shimada K, Yoshiyama M. Clinical significance of discrepant mid-wall late gadolinium enhancement in patients with nonischemic dilated cardiomyopathy. *Heart Vessels.* 2018 Dec 1;33:1482–9.
33. Messroghli DR, Moon JC, Ferreira VM, Grosse-Wortmann L, He T, Kellman P, et al. Clinical recommendations for cardiovascular magnetic resonance mapping of T1, T2, T2\* and extracellular volume: A consensus statement by the Society for Cardiovascular Magnetic Resonance (SCMR) endorsed by the European Association for Cardiovascular Imagi. *J Cardiovasc Magn Reson.* 2017 Dec;19:1–24.
34. Zhang Q, Werys K, Popescu IA, Biasioli L, Ntusi NAB, Desai M, et al. Quality assurance of quantitative cardiac T1-mapping in multicenter clinical trials – A T1 phantom program from the hypertrophic cardiomyopathy registry (HCMR) study. *Int J Cardiol.* 2021 May 1;330:251–8.
35. Liu CY, Liu YC, Wu C, Armstrong A, Volpe GJ, Van Der Geest RJ, et al. Evaluation

- of Age-Related Interstitial Myocardial Fibrosis With Cardiac Magnetic Resonance Contrast-Enhanced T1 Mapping: MESA (Multi-Ethnic Study of Atherosclerosis). *J Am Coll Cardiol*. 2013 Oct 1;62:1280–7.
36. Kersten J, Hackenbroch C, Bouly M, Tyl B, Bernhardt P. What Is Normal for an Aging Heart?: A Prospective CMR Cohort Study. *J Cardiovasc Imaging*. 2022 Jul 1;30:202.
  37. Roy C, Slimani A, De Meester C, Amzulescu M, Pasquet A, Vancraeynest D, et al. Age and sex corrected normal reference values of T1, T2 T2\*and ECV in healthy subjects at 3T CMR. *J Cardiovasc Magn Reson*. 2017 Sep 21;19:1–12.
  38. Powell-Wiley TM, Poirier P, Burke LE, Després J-P, Gordon-Larsen P, Lavie CJ, et al. Obesity and Cardiovascular Disease: A Scientific Statement From the American Heart Association. *Circulation*. 2021 May;143:E984–1010.
  39. Szabo L, McCracken C, Cooper J, Rider OJ, Vago H, Merkely B, et al. The role of obesity-related cardiovascular remodelling in mediating incident cardiovascular outcomes: a population-based observational study. *Eur Hear journal Cardiovasc Imaging*. 2023 Jan 20;1–9.
  40. Raisi-Estabragh Z, Gkontra P, Jaggi A, Cooper J, Augusto J, Bhuvana AN, et al. Repeatability of Cardiac Magnetic Resonance Radiomics: A Multi-Centre Multi-Vendor Test-Retest Study. *Front Cardiovasc Med*. 2020 Dec;7:1–16.

## TABLES

**Table 1. Baseline population characteristics**

	<b>Men</b>	<b>Women</b>
n	8,338	9,779
Age (years)	64.17 ( $\pm 7.50$ )	63.04 ( $\pm 7.36$ )
<b>Cardiac MRI metric</b>		
left ventricular end-diastolic volume index	82.83 ( $\pm 14.32$ )	73.50 ( $\pm 10.91$ )
Left ventricular mass index	50.94 ( $\pm 7.7$ )	40.66 ( $\pm 5.81$ )
Left ventricular ejection fraction	58.02 ( $\pm 5.99$ )	61.02 ( $\pm 5.59$ )
Right ventricular end-diastolic volume index	89.07 ( $\pm 15.16$ )	76.13 ( $\pm 11.89$ )
Right ventricular ejection fraction	55.28 ( $\pm 5.78$ )	59.25 ( $\pm 5.63$ )
<b>Socio-economic factors</b>		
Townsend score	-2.70[-3.93-0.62]	-2.55[-3.85-0.47]
<b>Education level:-</b>		
None	1[6.04%]	1 [5.84%]
Secondary education	2 [4.00%]	2 [3.92%]
High school diploma	3[16.87%]	3 [21.22%]
Vocational diploma	4[7.71%]	4 [3.24%]
Other professional qualifications eg: nursing, teaching	5[4.13%]	5 [6.20%]
A levels/AS levels or equivalent	6[11.85%]	6 [14.31%]
College or University degree	7 [49.41%]	7 [45.28%]
<b>Number of vehicles in household:-</b>		
1 None,	1 [3.24%]	1 [4.10%]
2 One,	2 [34.35%]	2 [39.39%]
3 Two,	3 [47.68%]	3 [43.47%]
4 Three,	4 [11.49%]	4 [9.95%]
5 Four or more,	5 [3.24%]	5 [3.09%]
<b>Average total household income before tax:-</b>		
1 Less than £18,000,	1 [8.92%]	1 [13.55%]
2 18,000 to 30,999	2 [20.30%]	2 [24.86%]
3 31,000 to 51,999	3 [31.63%]	3 [30.03%]
4 52,000 to 100,000	4 [31.15%]	4 [26.00%]
5 Greater than 100,000	5 [8.00%]	5 [5.55%]
Number of people in household	2.54[1.16]	2.48[1.15]
<b>Lifestyle factors</b>		
Time spent watching television (Hours/day)	2[1-3]	2[1-3]
<b>Oily fish intake:-</b>		
0= Never,	0 [9.22%]	0 [9.52%]
1= Less than once a week,	1 [36.14%]	1 [33.52%]
2= Once a week,	2 [37.61%]	2 [40.03%]
3= 2-4 times a week,	3 [15.99%]	3 [16.38%]
4= 5-6 times a week,	4 [0.81%]	4 [0.49%]
5= Once or more daily	5 [0.22%]	5 [0.05%]
<b>Beef intake:-</b>		
0= Never,	0 [7.38%]	0 [13.54%]
1= Less than once a week,	1 [47.06%]	1 [45.55%]

2= Once a week,	2 [33.88%]	2 [29.58%]
3= 2-4 times a week,	3 [11.48%]	3 [11.25%]
4= 5-6 times a week,	4 [0.16%]	4 [0.06%]
5= Once or more daily	5 [0.04%]	5 [0.01%]
Pork intake:-		
0= Never,	0 [11.67%]	0 [19.49%]
1= Less than once a week,	1 [60.84%]	1 [59.35%]
2= Once a week,	2 [23.65%]	2 [18.74%]
3= 2-4 times a week,	3 [3.71%]	3 [2.38%]
4= 5-6 times a week,	4 [0.10%]	4 [0.04%]
5= Once or more daily	5 [0.02%]	5[0%]
Number of days/week of moderate physical activity 10+ minutes (days/week)	3.33[2.24]	3.50[2.28]
Smoking status		
0, Never	0 [56.05%]	0 [63.87%]
1, Previous	1 [36.81%]	1 [31.19%]
2, Current	2 [7.14%]	2 [4.94%]
Obesity and body composition metrics		
Visceral adipose tissue volume (Litres)	4.77[3.33 -6.49]	2.37[1.51-3.57]
Abdominal subcutaneous adipose tissue volume (Litres)	5.53[4.29-7.16]	7.59[5.66-9.94]
Total trunk fat volume (Litres)	10.97[4.29]	10.71[4.61]
Body mass index (kg/m <sup>2</sup> )	26.85[24.76-29.37]	25.43[23.09-28.85]
Whole body fat mass (kg)	21.45[7.23]	25.74[8.88]
Waist circumference (cm)	95.13[10.26]	82.51[11.13]
Liver PDFF (proton density fat fraction, %)	2.92[1.80-6.13]	1.98[1.33-3.81]
Total lean tissue volume (Litres)	27.38[25.77-29.87]	20.25[18.60-22.14]
Trunk fat mass (kg)	14.02[4.54]	13.23[4.84]
Blood pressure and arterial stiffness		
Pulse rate (bpm)	67[60-74]	68[62-75]
Pulse wave Arterial Stiffness index (m/s)	9.63[7.72-11.83]	8.12[6.20-10.33]
Diastolic blood pressure, automated reading (mmHg)	84.10[9.93]	79.88[10.28]
Systolic blood pressure, automated reading (mmHg)	141.31[16.81]	134.19[18.99]
Blood biomarkers		
Alanine aminotransferase (units per Litre)	23.97[18.63-32.18]	17.19[13.62-22.47]
Gamma glutamyltransferase (units per Litre)	31.90[23.10-47.30]	20.25[15.30-28.80]
Glycated haemoglobin (mmol/mol)	34.80[32.40-37.30]	34.60[32.30-37.10]
Triglycerides Level (mmol/L)	1.67[1.18-2.38]	1.27[0.93-1.78]
Cholesterol (mmol/L)	5.55[1.07]	5.86[1.07]
LDL (mmol/L)	3.54[0.83]	3.62[0.83]
HDL (mmol/L)	1.26[1.08-1.46]	1.58[1.35-1.83]
Mental health		
Fed-up feelings:-		
1 Yes,	1 [33.78%]	1 [40.13%]
0 No	0 [66.22%]	0 [59.87%]
Nervous feelings:-		
1 Yes,	1 [18.22%]	1 [23.98%]

0 No	0 [81.78%]	0 [76.02%]
Neuroticism score	3.52[3.17]	4.47[3.20]
Health satisfaction:-		
1-Extremely unhappy,	1 [0.34%]	1 [0.74%]
2-Very unhappy,	2 [1.47%]	2 [1.67%]
3-Moderately unhappy,	3 [7.11%]	3 [7.94%]
4-Moderately happy,	4 [48.69%]	4 [48.59%]
5-Very happy,	5 [37.07%]	5 [35.93%]
6-Extremely happy,	6 [5.32%]	6 [5.12%]
Financial situation satisfaction:-		
1-Extremely unhappy,	1 [0.73%]	1 [0.90%]
2-Very unhappy,	2 [1.77%]	2 [1.67%]
3-Moderately unhappy,	3 [5.19%]	3 [5.59%]
4-Moderately happy,	4 [38.55%]	4 [37.86%]
5-Very happy,	5 [41.06%]	5 [41.84%]
6-Extremely happy,	6 [12.71%]	6 [12.14%]
Ever unenthusiastic/disinterested for a whole week		
1-Yes,	1 [29.89%]	1 [41.47%]
0-No,	0 [70.11%]	0 [58.53%]
Multi-organ health indicators		
Number of treatments/medications taken	2[0-3]	2[1-4]
Overall health rating:-		
1-Poor,	1 [1.86%]	1 [2.17%]
2-Fair,	2 [17.69%]	2 [15.73%]
3-Good,	3 [61.81%]	3 [63.30%]
4-Excellent	4 [18.63%]	4 [18.79%]
Fluid intelligence score	6.67[2.14]	6.39[1.94]
Mouth/teeth dental problems:-		
0 No,	0 [66.58%]	0 [63.23%]
1 Yes (Mouth ulcers, Painful gums, Bleeding gums, Loose teeth, Toothache, Dentures,	1 [33.42%]	1 [36.77%]
Heel bone mineral density (g/m2)	0.58[0.14]	0.53[0.12]
Hand grip strength (left, kg)	40[34-46]	24[20-28]
Hand grip strength (right, kg))	42[36-48]	26[22-30]
Forced expiratory volume in 1-second (FEV1), Best measure (litres)	3.42[0.68]	2.50[0.50]
Forced vital capacity (FVC, litres)	4.54[1.06]	3.24[0.61]
Peak expiratory flow (PEF, litres/min)	502[427-573]	350[300-400]
Sex hormones		
Oestradiol	202.30[187.45-223.15]	410.7 [275.5 - 674.3]
Testosterone	13.12[10.9-15.4]	1.1[0.9-1.5]

**Table 1 footnote.** Discrete variables are presented as number (percentage). Continuous measures are mean ( $\pm$ SD) if normal distribution. Continuous measures are median [25th percentile, 75th percentile] if skewed distribution. **Note:** All individuals with answers: don't know (-1) & prefer not to answer (-3) were removed. MRI: Magnetic resonance imaging.

**Table 2. Summary of model performance metrics**

Women					
	LV	RV	MYO	LA	RA
Mean MAE (years)	4.96	5.26	5.10	5.10	5.07
Mean Predicted R <sup>2</sup>	0.29	0.20	0.24	0.24	0.26
Correlation between predicted cardiac structure age and actual age	0.90	0.92	0.91	0.91	0.91
Men					
	LV	RV	MYO	LA	RA
Mean MAE (years)	5.33	5.49	5.42	5.36	5.37
Mean Predicted R <sup>2</sup>	0.22	0.17	0.19	0.21	0.20
Correlation between predicted cardiac structure age and actual age	0.92	0.93	0.93	0.92	0.92

**Table 2 footnote.** LA: left atrium; LV: left ventricle; MAE: mean absolute error; MYO: myocardium; RA: right atrium; RV: right ventricle. \*Reported performance metrics are prior to application of the regression to the mean correction.

**Table 3. The number of significant associations in each of the five regions separated by sex.**

Sex	LA	LV	MYO	RA	RV	Total
Men	7	23	27	9	17	83
Women	8	22	25	11	23	89
Total	15	45	52	20	40	172

**Table 3 footnote.** LA: left atrium; LV: left ventricle; MYO: myocardium; RA: right atrium; RV: right ventricle.

**Table 4. The number of significant associations in each of the exposure group separated by sex and cardiac structures.**

Exposures groups	Sex	LA	LV	MYO	RA	RV	Total	
Blood Biomarkers (n= 7)	Men	1	1	3	0	0	5	21
	Women	2	2	5	2	5	16	
Blood pressure and arterial stiffness (n= 4)	Men	1	2	3	2	2	10	24
	Women	0	4	4	2	4	14	
Lifestyle (n= 6)	Men	0	1	2	0	2	5	7
	Women	0	2	0	0	0	2	
Mental well-being (n= 6)	Men	0	4	4	2	5	15	21
	Women	2	1	2	0	1	6	
Multi-organ health indicators (n= 10)	Men	3	6	5	5	1	20	40
	Women	3	5	6	1	5	20	
Obesity and body composition metrics (n= 9)	Men	0	8	8	0	7	23	51
	Women	0	7	7	6	8	28	
Socio-economic (n= 5)	Men	2	0	2	0	0	4	7
	Women	1	1	1	0	0	3	
Sex hormones (n= 2)	Men	0	1	0	0	0	1	1
	Women	0	0	0	0	0	0	

**Table 4 footnote.** LA: left atrium; LV: left ventricle; MYO: myocardium; RA: right atrium; RV: right ventricle.

## FIGURE LEGENDS

**Figure 1.** Conceptual overview of the steps used to estimate heart age for each cardiac region and perform PheWAS

**Figure 1 footnote.** These steps were performed separately for women and men. LA: left atrium; LV: left ventricle; MYO: myocardium; PheWAS: phenome wide association study; RA: right atrium; RV: right ventricle. The full list of exposures is presented in Supplementary table 4

**Figure 2.** Top 10 more informative features for heart age models of left heart cardiac region for men and women, as identified by SHAP values

**Figure 2 footnote.** The x axis indicates the SHAP value range of each feature while the y axis displays the feature name. Each dot or circle in the plot indicates one subject in the model while the color shows how that feature is associated with the outcome. Red color indicates positive correlation while the blue color means negative correlation. A Zero SHAP value means the feature does not affect the outcome of the model. Asterisk indicates features extracted at end systole. SHAP: SHapley Additive exPlanations; GLCM: Gray Level Co-occurrence Matrix; GLDM: Gray Level Dependence Matrix; GLRLM: Gray Level Run Length Matrix; GLSZM: Gray Level Size Zone Matrix.

**Figure 3.** Top 10 more informative features for heart age models of right heart cardiac region for men and women, as identified by SHAP values

**Figure 3 footnote.** The x axis indicates the SHAP value range of each feature while the y axis displays the feature name. Each dot or circle in the plot indicates one subject in the model while the color shows how that feature is associated with the outcome. Red color indicates positive correlation while the blue color means negative correlation. A Zero SHAP value means the feature does not affect the outcome of the model. Asterisk indicates features extracted at end



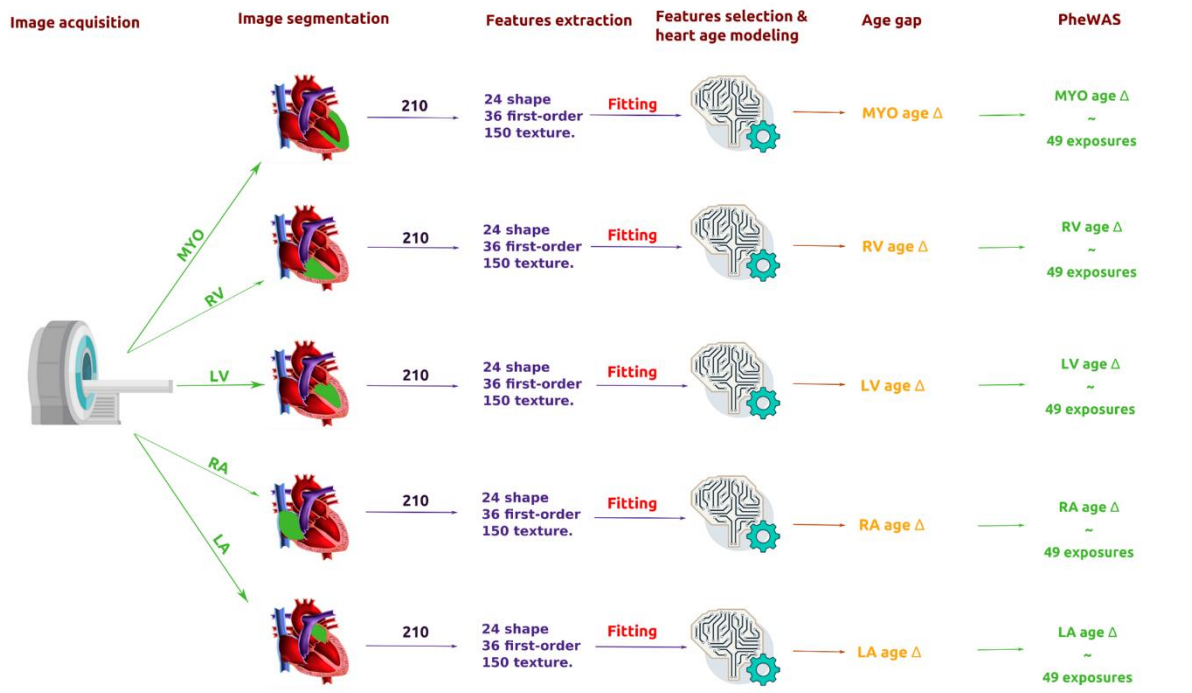
systole. SHAP: SHapley Additive exPlanations; GLCM: Gray Level Co-occurrence Matrix; GLDM: Gray Level Dependence Matrix; GLRLM: Gray Level Run Length Matrix; GLSZM: Gray Level Size Zone Matrix; NGTDM: Neighbouring Gray Tone Difference Matrix.

**Figure 4.** Association of all exposures with heart age gap in the five cardiac regions modelled for men and women

**Figure 4 footnote.** The x axis represents the coefficient value of the association of each exposure with the cardiac age gap while the y axis represents the exposure names. The coefficient values (beta) are not standardized which means every one unit increasing or decreasing in these exposures (independent variables) lead to increasing or decreasing in the heart age gap (dependent variable) in years based on the beta value when all other exposures are constant. Exposures with asterisk are statistically significant (corrected p-value < 0.05). Please refer to Supplementary Table 3 for full explanation of each exposure and its measurement units. BMD: Heel bone mineral density; HDLC: HDL cholesterol; FVC: Forced vital capacity; OHR: Overall health rating; FEV1: Forced expiratory volume in 1-second, Best measure; HeSa: Health satisfaction; ASAT: Abdominal subcutaneous adipose tissue volume; TLTV: Total lean tissue volume; NeFe: Nervous feelings; NinH: Number in household; LDLD: LDL direct; OFiI: Oily fish intake; SmSt: Smoking status; FSS: Financial situation satisfaction; CHOL: Cholesterol; Uu/Di: Ever unenthusiastic/ disinterested for a whole week ; ATHI: Average total household income before tax; NVH: Number of vehicles in household; NMPA: Number of days/week of moderate physical activity 10+ minutes; TriL: Triglycerides Level; TFM: Trunk fat mass; MTDP: Mouth/teeth dental problems; PorI: Pork intake; BMI: Body mass index; FUF: Fed-up feelings; EDUL: Education level; TowS: Townsend score; PWAS: Pulse wave Arterial Stiffness index (m/s); BEEI: Beef\_intake; FIS: Fluid intelligence score; HGSL: Hand grip strength (left); PDFF: 10P Liver PDFF (proton density fat fraction); TTFV: Total trunk fat volume; TSWT: Time spent watching television; NTMT: Number of

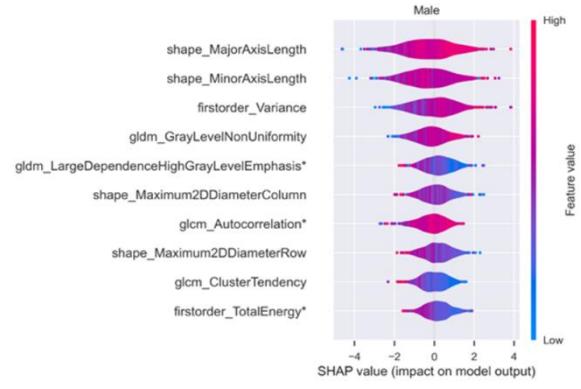
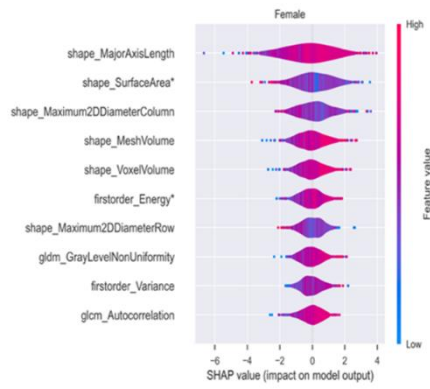
treatments/medications taken; HGSR: Hand grip strength (right); HbA1c: Glycated haemoglobin; WBFM: Whole body fat mass; SBP: Systolic blood pressure, automated reading (mmHg); ALAM: Alanine aminotransferase; DBP: Diastolic blood pressure, automated reading (mmHg); PulR: Pulse rate; NeSc: Neuroticism score; PEF: Peak expiratory flow; GaGl: Gamma glutamyltransferase; GaGl: Gamma glutamyltransferase; WaiC: Waist circumference; VATV: Visceral adipose tissue volum.

Figure 1

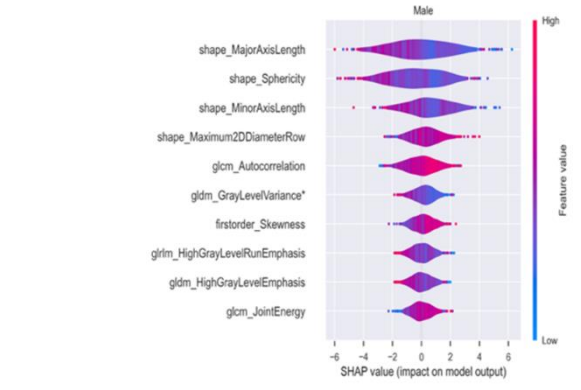
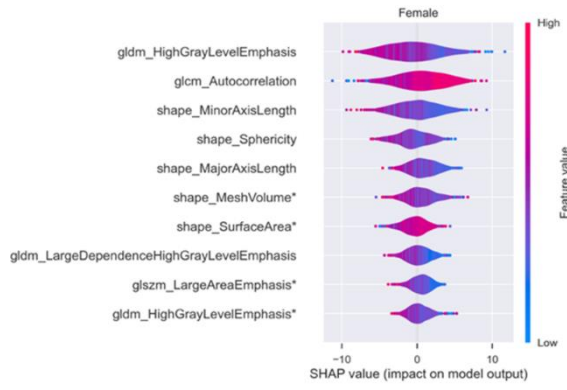


**Figure 2**

LA



LV



MYO

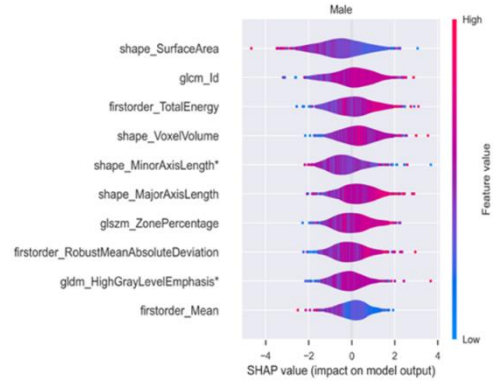
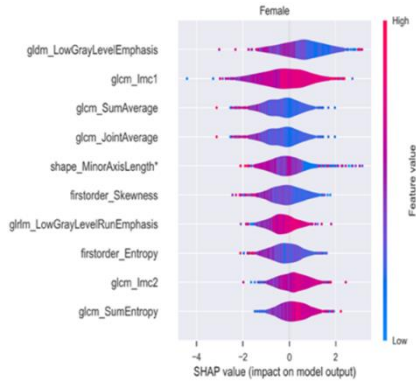


**Figure 3**

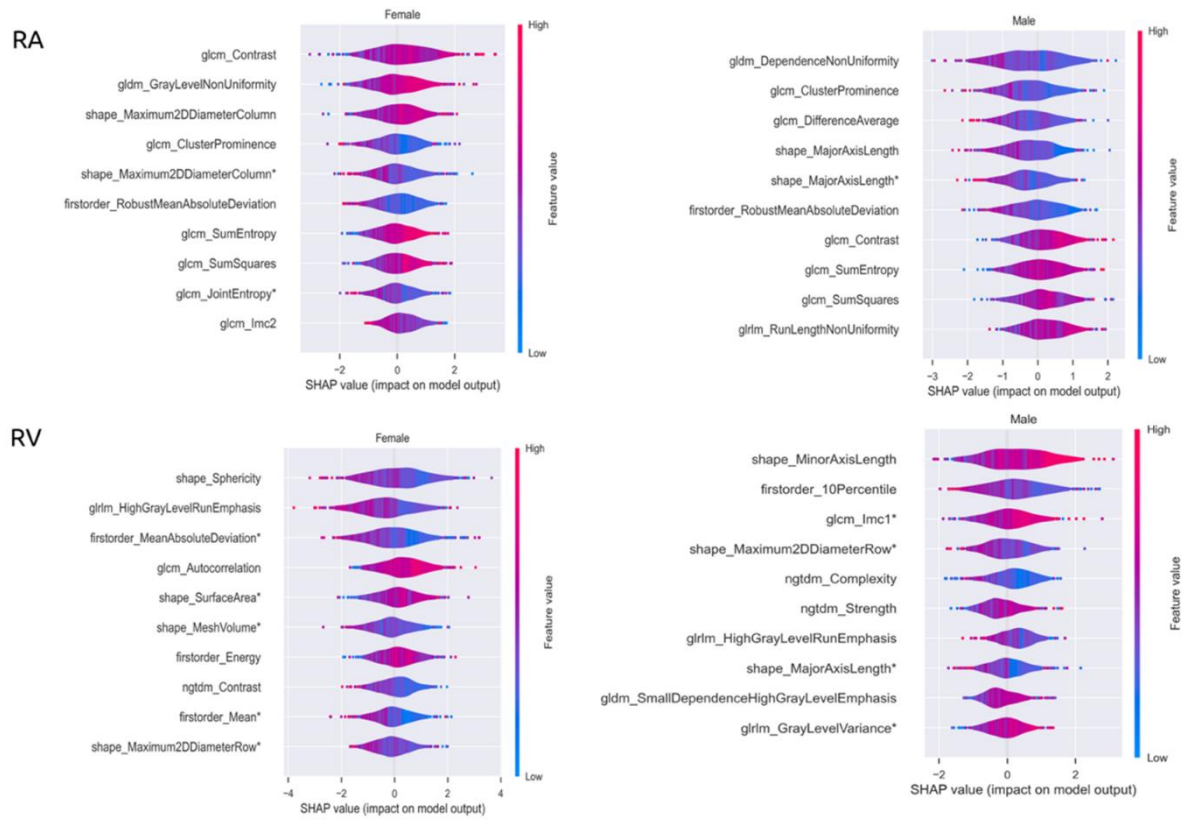
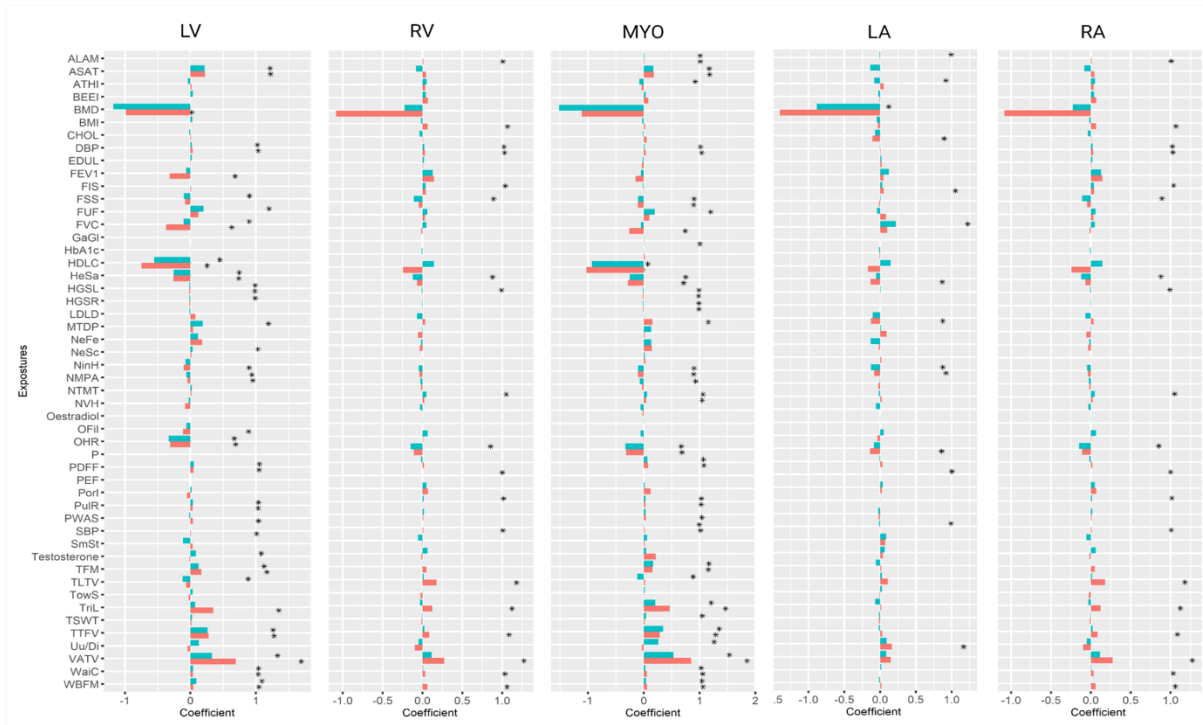


Figure 4



**SUPPLEMENTAL MATERIALS**

**Supplementary Table 1: Approach to ascertainment of cardiac diseases**

Variable	UK Biobank field ID	Condition
Self-report	20002	Angina
		Heart attack/myocardial infarction
		Mitral stenosis
		Mitral valve disease
		Heart valve problem/heart murmur
		Mitral regurgitation / incompetence
		Aortic valve disease
		Aortic stenosis
		Aortic regurgitation / incompetence
		Cardiomyopathy
		Hypertrophic cardiomyopathy (HCM / HOCM)
		Heart failure/pulmonary odema
		Sick sinus syndrome
		Supraventricular tachycardia
		Atrial fibrillation
		Atrial flutter
		Heart arrhythmia
Irregular heart beat		
ICD-10	41202	Angina pectoris
		Other acute ischaemic heart diseases
		Chronic ischaemic heart disease
		Acute myocardial infarction
		Subsequent myocardial infarction
		Certain current complications following acute myocardial infarction
		Mitral (valve) insufficiency
		Nonrheumatic mitral (valve) stenosis
		Other nonrheumatic mitral valve disorders
		Non-rheumatic mitral valve disorder, unspecified
		Non-rheumatic aortic valve disorders
		Non-rheumatic tricuspid valve disorders
		Pulmonary valve disorders
		Endocarditis, valve unspecified
		Mitral valve disorders in diseases classified elsewhere
		Aortic valve disorders in diseases classified elsewhere
		Pulmonary valve disorders in diseases classified elsewhere
		Multiple valve disorders in diseases classified elsewhere
		Endocarditis, valve unspecified, in diseases classified elsewhere
		Cardiomyopathy
		Cardiomyopathy in diseases classified elsewhere
		Congestive heart failure
		Left ventricular failure
		Heart failure, unspecified
		Atrioventricular block, second degree
		Atrioventricular block, complete
		Trifascicular block
		Preexcitation syndrome
		Cardiac arrest with successful resuscitation
		Sudden cardiac death, so described
		Cardiac arrest, unspecified
		Re-entry ventricular arrhythmia



		Supraventricular tachycardia
		Ventricular tachycardia
		Paroxysmal tachycardia, unspecified
		Paroxysmal atrial fibrillation
		Persistent atrial fibrillation
		Chronic atrial fibrillation
		Typical atrial flutter
		Atypical atrial flutter
		Atrial fibrillation and atrial flutter, unspecified
		Ventricular fibrillation and flutter
		Sick sinus syndrome
		Rheumatic mitral valve diseases
		Rheumatic aortic valve diseases
		Rheumatic tricuspid valve diseases
		Multiple valve diseases
		Hypertensive heart disease
		Hypertensive heart and renal disease
ICD-9	41203	Coronary atherosclerosis
		Other specified forms of chronic ischaemic heart disease
		Chronic ischaemic heart disease, unspecified
		Acute myocardial infarction
		Other acute and subacute forms of ischaemic heart disease
		Old myocardial infarction
Algorithm	42000	Date of myocardial infarction
Diagnosed by doctor	6150	Angina
	3627	Age angina diagnosed
	6150	Heart attack
	3894	Age heart attack diagnosed
First occurrences	131296	Angina pectoris
	131304	Other acute ischaemic heart diseases
	131306	Chronic ischaemic heart disease
	131298	Acute myocardial infarction
	131300	Subsequent myocardial infarction
	131302	Certain current complications following acute myocardial infarction
	131322	Nonrheumatic mitral valve disorders
	131324	Nonrheumatic aortic valve disorders
	131326	Nonrheumatic tricuspid valve disorders
	131328	Pulmonary valve disorders
	131330	Endocarditis, valve unspecified
	131332	Endocarditis and heart valve disorders in diseases classified elsewhere
	131338	Cardiomyopathy
	131340	Cardiomyopathy in diseases classified elsewhere
	131346	Cardiac arrest
	131348	Paroxysmal tachycardia
	131350	Atrial fibrillation and flutter
	131276	Rheumatic mitral valve diseases
	131278	Rheumatic aortic valve diseases
	131280	Rheumatic tricuspid valve diseases
	131282	Multiple valve diseases
	131288	Hypertensive heart disease

	131292	Hypertensive heart and renal disease
	131354	Heart failure

**Supplementary Table 1 footnote.** ICD: international classification of disease.

**Supplementary Table 2. List of radiomic features used to estimate cardiac age**

shape_Elongation	glcm_SumEntropy
shape_MajorAxisLength	glcm_SumSquares
shape_Maximum2DDiameterColumn	gldm_DependenceEntropy
shape_Maximum2DDiameterRow	gldm_DependenceNonUniformity
shape_Maximum2DDiameterSlice	gldm_DependenceNonUniformityNormalized
shape_Maximum3DDiameter	gldm_DependenceVariance
shape_MeshVolume	gldm_GrayLevelNonUniformity
shape_MinorAxisLength	gldm_GrayLevelVariance
shape_Sphericity	gldm_HighGrayLevelEmphasis
shape_SurfaceArea	gldm_LargeDependenceEmphasis
shape_SurfaceVolumeRatio	gldm_LargeDependenceHighGrayLevelEmphasis
shape_VoxelVolume	gldm_LargeDependenceLowGrayLevelEmphasis
firstorder_10Percentile	gldm_LowGrayLevelEmphasis
firstorder_90Percentile	gldm_SmallDependenceEmphasis
firstorder_Energy	gldm_SmallDependenceHighGrayLevelEmphasis
firstorder_Entropy	gldm_SmallDependenceLowGrayLevelEmphasis
firstorder_InterquartileRange	glrlm_GrayLevelNonUniformity
firstorder_Kurtosis	glrlm_GrayLevelNonUniformityNormalized
firstorder_Maximum	glrlm_GrayLevelVariance
firstorder_MeanAbsoluteDeviation	glrlm_HighGrayLevelRunEmphasis
firstorder_Mean	glrlm_LongRunEmphasis
firstorder_Median	glrlm_LongRunHighGrayLevelEmphasis
firstorder_Minimum	glrlm_LongRunLowGrayLevelEmphasis
firstorder_Range	glrlm_LowGrayLevelRunEmphasis
firstorder_RobustMeanAbsoluteDeviation	glrlm_RunEntropy
firstorder_RootMeanSquared	glrlm_RunLengthNonUniformity
firstorder_Skewness	glrlm_RunLengthNonUniformityNormalized
firstorder_TotalEnergy	glrlm_RunPercentage
firstorder_Uniformity	glrlm_RunVariance
firstorder_Variance	glrlm_ShortRunEmphasis
glcm_Autocorrelation	glrlm_ShortRunHighGrayLevelEmphasis
glcm_ClusterProminence	glrlm_ShortRunLowGrayLevelEmphasis
glcm_ClusterShade	glszm_GrayLevelNonUniformity
glcm_ClusterTendency	glszm_GrayLevelNonUniformityNormalized
glcm_Contrast	glszm_GrayLevelVariance
glcm_Correlation	glszm_HighGrayLevelZoneEmphasis
glcm_DifferenceAverage	glszm_LargeAreaEmphasis
glcm_DifferenceEntropy	glszm_LargeAreaHighGrayLevelEmphasis
glcm_DifferenceVariance	glszm_LargeAreaLowGrayLevelEmphasis
glcm_Id	glszm_LowGrayLevelZoneEmphasis
glcm_Idm	glszm_SizeZoneNonUniformity
glcm_Idmn	glszm_SizeZoneNonUniformityNormalized
glcm_Idn	glszm_SmallAreaEmphasis
glcm_Imc1	glszm_SmallAreaHighGrayLevelEmphasis
glcm_Imc2	glszm_SmallAreaLowGrayLevelEmphasis
glcm_InverseVariance	glszm_ZoneEntropy
glcm_JointAverage	glszm_ZonePercentage
glcm_JointEnergy	glszm_ZoneVariance
glcm_JointEntropy	ngtdm_Busyness
glcm_MCC	ngtdm_Coarseness
glcm_MaximumProbability	ngtdm_Complexity

glcm_SumAverage	ngtdm_Contrast
	ngtdm_Strength

**Supplementary Table 2 footnote.** Each feature was extracted twice (end-systole, end-diastole) from each cardiac region resulting in a total of 210 features for each region. GLCM: gray-level co-occurrence matrix; GLRLM: gray-level run-length matrix; GLSZM: gray-level size-zone matrix; NGTDM: neighboring gray tone difference matrix; GLDM: gray-level dependence matrix.

**Supplementary Table 3: Number of features and subjects included in modelling for each region of interest after feature selection and outlier removal procedures**

Women					
	LV	RV	MYO	LA	RA
Original number of features	210				
Optimal number of features using RFECV	125	91	121	102	65
Original number of subjects	15095				
Number of subjects free of heart diseases	9779				
Final number of subjects after applying outliers' removal	9402	9402	9416	9419	9409
Men					
	LV	RV	MYO	LA	RA
Original number of features	210				
Optimal number of features using RFECV	118	95	43	91	58
Original number of subjects	14049				
Number of subjects free of heart diseases	8338				
Final number of subjects after applying outliers' removal	8040	8051	8049	8065	8070

**Supplementary Table 3 footnote.** LA: left atrium; LV: left ventricle; MYO: myocardium; RA: right atrium; RV: right ventricle; RFECV: recursive feature elimination with cross-validation.

**Supplementary Table 4. Associations of all exposures with heart age gap from the five cardiac regions modelled**

Coefficient	Sex	Anatomy	P-value	Exposures
-1.51788	Male	MYO	7.44E-06	Heel bone mineral density (BMD)
-1.39966	Female	LA	5.29E-04	Heel bone mineral density (BMD)
-1.17606	Male	LV	2.26E-03	Heel bone mineral density (BMD)
-1.11439	Female	MYO	3.14E-03	Heel bone mineral density (BMD)
-1.08438	Female	RA	2.37E-02	Heel bone mineral density (BMD)
-1.02737	Female	MYO	7.71E-21	HDL cholesterol
-0.98516	Female	LV	1.66E-02	Heel bone mineral density (BMD)
-0.92931	Male	MYO	3.55E-13	HDL cholesterol
-0.88149	Male	LA	2.85E-02	Heel bone mineral density (BMD)
-0.74638	Female	RV	4.35E-02	Heel bone mineral density (BMD)
-0.74552	Female	LV	1.65E-10	HDL cholesterol
-0.66669	Male	RV	8.73E-02	Heel bone mineral density (BMD)
-0.55235	Male	LV	1.80E-04	HDL cholesterol
-0.52283	Female	RV	6.23E-07	HDL cholesterol
-0.37027	Female	LV	1.62E-07	Forced vital capacity (FVC)
-0.33161	Male	LV	3.53E-09	Overall health rating
-0.33055	Male	MYO	2.88E-10	Overall health rating
-0.31878	Female	MYO	1.40E-09	Overall health rating
-0.31826	Female	LV	1.44E-03	Forced expiratory volume in 1-second (FEV1), Best measure
-0.31065	Female	LV	3.72E-08	Overall health rating
-0.31039	Male	RV	6.88E-02	HDL cholesterol
-0.28894	Female	MYO	1.93E-11	Health satisfaction
-0.26208	Female	LV	1.73E-08	Health satisfaction
-0.26087	Female	MYO	2.03E-04	Forced vital capacity (FVC)
-0.25658	Male	LV	1.57E-07	Health satisfaction
-0.25254	Male	MYO	3.76E-08	Health satisfaction
-0.24338	Female	RA	5.91E-02	HDL cholesterol
-0.23725	Male	RV	7.66E-06	Overall health rating
-0.23346	Female	RV	4.98E-06	Overall health rating
-0.22582	Male	RA	5.47E-01	Heel bone mineral density (BMD)
-0.21006	Female	RV	2.13E-02	Forced expiratory volume in 1-second (FEV1), Best measure
-0.17409	Male	RV	1.81E-04	Health satisfaction
-0.17015	Female	LA	1.99E-01	HDL cholesterol
-0.14991	Female	MYO	1.15E-01	Forced expiratory volume in 1-second (FEV1), Best measure
-0.14897	Female	RV	7.75E-04	Health satisfaction
-0.14705	Male	RA	1.51E-02	Overall health rating
-0.14154	Female	LA	1.54E-02	Overall health rating
-0.13961	Male	LA	1.93E-01	Abdominal subcutaneous adipose tissue volume
-0.13593	Male	RV	8.29E-05	Total lean tissue volume
-0.13376	Female	LA	8.60E-03	Health satisfaction
-0.1296	Male	LA	4.60E-01	Nervous feelings
-0.12773	Female	RV	5.17E-02	Forced vital capacity (FVC)
-0.12686	Male	LA	3.61E-04	Number in household

-0.12681	Female	LA	1.63E-02	LDL direct
-0.12084	Male	RA	2.28E-02	Health satisfaction
-0.11941	Male	LV	1.34E-03	Total lean tissue volume
-0.11917	Male	MYO	7.04E-04	Total lean tissue volume
-0.11265	Female	LV	1.22E-02	Oily fish intake
-0.11152	Male	LV	8.68E-02	Smoking status
-0.10913	Female	MYO	3.08E-03	Number in household
-0.1088	Female	MYO	1.11E-02	Financial situation satisfaction
-0.1084	Male	RA	2.28E-02	Financial situation satisfaction
-0.10796	Female	RA	1.14E-01	Overall health rating
-0.10623	Female	LA	1.57E-02	Cholesterol
-0.10468	Female	LV	8.63E-03	Number in household
-0.10392	Male	LA	7.75E-02	LDL direct
-0.10277	Male	LV	2.62E-02	Forced vital capacity (FVC)
-0.10262	Male	MYO	3.14E-03	Number in household
-0.10195	Male	MYO	9.93E-03	Financial situation satisfaction
-0.09994	Male	LV	1.87E-02	Financial situation satisfaction
-0.09562	Female	RA	4.58E-01	Ever unenthusiastic/disinterested for a whole week
-0.095	Male	RV	1.04E-02	Financial situation satisfaction
-0.08802	Female	RV	3.31E-02	Total lean tissue volume
-0.08728	Male	LA	1.42E-01	Overall health rating
-0.08236	Female	LV	7.50E-02	Financial situation satisfaction
-0.08224	Male	LA	3.18E-02	Average total household income before tax
-0.08182	Female	LA	4.83E-02	Number in household
-0.08132	Female	LV	9.87E-02	Number of vehicles in household
-0.08122	Male	RA	8.15E-01	Abdominal subcutaneous adipose tissue volume
-0.08046	Male	MYO	2.39E-02	Average total household income before tax
-0.07284	Male	LV	5.79E-02	Number in household
-0.07158	Male	MYO	5.04E-06	Number of days/week of moderate physical activity 10+ minutes
-0.06936	Female	RA	4.58E-01	Health satisfaction
-0.06776	Female	RV	7.69E-02	Oily fish intake
-0.06762	Male	RV	1.38E-01	Number of vehicles in household
-0.0672	Male	RA	4.08E-01	LDL direct
-0.06705	Male	LA	9.87E-02	Triglycerides Level
-0.06692	Female	LV	1.65E-01	Total lean tissue volume
-0.06683	Male	LA	9.59E-02	Cholesterol
-0.06426	Male	LV	3.54E-01	Forced expiratory volume in 1-second (FEV1), Best measure
-0.06389	Male	LV	1.48E-01	Oily fish intake
-0.06373	Male	RV	7.11E-02	Number in household
-0.06278	Male	LV	2.87E-04	Number of days/week of moderate physical activity 10+ minutes
-0.0592	Male	MYO	2.21E-01	Number of vehicles in household
-0.05888	Male	LA	3.81E-01	Trunk fat mass
-0.05866	Male	LA	2.16E-01	Number of vehicles in household
-0.05742	Male	MYO	2.30E-01	Oily fish intake
-0.05595	Male	LA	4.60E-01	Health satisfaction

-0.05535	Female	RA	5.95E-01	Mouth/teeth dental problems
-0.05496	Male	RA	4.23E-01	Smoking status
-0.05114	Male	MYO	2.51E-01	Forced vital capacity (FVC)
-0.05054	Male	MYO	4.02E-01	Forced expiratory volume in 1-second (FEV1), Best measure
-0.04976	Male	RA	7.64E-01	Ever unenthusiastic/disinterested for a whole week
-0.0492	Female	LV	4.87E-01	Pork intake
-0.04887	Male	RV	3.04E-03	Number of days/week of moderate physical activity 10+ minutes
-0.04792	Female	LV	9.75E-03	Number of days/week of moderate physical activity 10+ minutes
-0.04781	Female	RV	2.51E-01	Financial situation satisfaction
-0.047	Male	RA	3.34E-01	Number in household
-0.04639	Male	LA	3.98E-01	Body mass index
-0.04586	Female	RA	4.58E-01	Financial situation satisfaction
-0.04369	Male	LA	8.32E-01	Fed-up feelings
-0.0418	Female	LV	5.58E-01	Ever unenthusiastic/disinterested for a whole week
-0.04022	Male	RV	6.48E-01	Smoking status
-0.04	Female	MYO	3.36E-01	Average total household income before tax
-0.03887	Female	MYO	5.66E-01	Ever unenthusiastic/disinterested for a whole week
-0.03859	Female	LA	4.50E-01	Oily fish intake
-0.03811	Male	LV	3.25E-01	Average total household income before tax
-0.03676	Female	RA	4.63E-01	Number in household
-0.03588	Male	RA	4.08E-01	Cholesterol
-0.03545	Female	MYO	9.43E-02	Education level
-0.03415	Female	RA	8.01E-01	Nervous feelings
-0.03325	Female	RV	8.81E-02	Education level
-0.03246	Male	RA	4.33E-01	Triglycerides Level
-0.03099	Male	RA	5.78E-01	Number of vehicles in household
-0.03061	Female	MYO	7.75E-02	Number of days/week of moderate physical activity 10+ minutes
-0.02994	Female	LA	4.71E-01	Body mass index
-0.02902	Male	LV	5.02E-01	Number of vehicles in household
-0.02847	Female	LV	7.95E-02	Townsend score
-0.02833	Male	LA	2.11E-01	Pulse wave Arterial Stiffness index (m/s)
-0.02726	Male	RV	3.63E-01	Average total household income before tax
-0.02699	Female	LA	1.85E-01	Number of days/week of moderate physical activity 10+ minutes
-0.02687	Female	RV	8.81E-02	Townsend score
-0.02619	Male	MYO	4.27E-01	Body mass index
-0.02575	Male	LA	6.58E-01	Beef intake
-0.02514	Female	MYO	6.75E-01	Number of vehicles in household
-0.02496	Male	RA	2.97E-01	Number of days/week of moderate physical activity 10+ minutes
-0.02457	Female	RA	2.82E-01	Townsend score
-0.02456	Male	RV	6.48E-01	Oily fish intake
-0.0241	Male	RV	6.48E-01	Beef intake
-0.02117	Male	RV	2.26E-01	Fluid intelligence score
-0.02081	Female	MYO	3.44E-04	Hand grip strength (left)
-0.02042	Male	MYO	2.21E-01	Education level



-0.02037	Female	LA	2.64E-01	Pulse wave Arterial Stiffness index (m/s)
-0.02021	Male	RA	8.15E-01	Liver PDFF (proton density fat fraction)
-0.01972	Male	RA	9.29E-01	Nervous feelings
-0.01845	Female	RV	7.43E-01	Number in household
-0.01814	Female	RA	3.27E-01	Number of days/week of moderate physical activity 10+ minutes
-0.01775	Male	LA	6.64E-01	Total trunk fat volume
-0.01773	Female	LA	1.85E-01	Time spent watching television
-0.01771	Male	LA	3.90E-01	Number of treatments/medications taken
-0.01744	Male	LV	8.41E-01	Cholesterol
-0.01714	Male	RA	8.51E-01	Body mass index
-0.01705	Male	MYO	7.01E-01	Cholesterol
-0.01653	Female	LA	8.32E-01	Nervous feelings
-0.01607	Male	MYO	9.93E-05	Hand grip strength (right)
-0.01597	Male	LV	4.33E-01	Pulse wave Arterial Stiffness index (m/s)
-0.01587	Male	MYO	3.41E-01	Fluid intelligence score
-0.01524	Female	RV	7.69E-03	Hand grip strength (left)
-0.01502	Female	RV	7.69E-03	Hand grip strength (right)
-0.014996	Female	RA	8.80E-01	Testosterone
-0.01498	Male	RV	3.63E-01	Education level
-0.01495	Female	LV	1.66E-02	Hand grip strength (left)
-0.01481	Female	RA	8.21E-01	Forced vital capacity (FVC)
-0.01445	Female	MYO	9.89E-03	Hand grip strength (right)
-0.01441	Female	LA	8.32E-01	Financial situation satisfaction
-0.01416	Male	MYO	7.38E-04	Hand grip strength (left)
-0.01402	Female	LV	9.85E-01	Testosterone
-0.0139	Male	LA	8.43E-02	Glycated haemoglobin (HbA1c)
-0.01383	Male	LA	4.20E-01	Time spent watching television
-0.01332	Female	RV	3.88E-01	Number of days/week of moderate physical activity 10+ minutes
-0.01329	Female	RA	3.27E-01	Time spent watching television
-0.01174	Male	LV	8.41E-01	LDL direct
-0.01157	Male	LV	1.63E-02	Hand grip strength (left)
-0.01151	Male	LA	6.64E-01	Whole body fat mass
-0.01122	Male	LA	2.26E-07	Systolic blood pressure, automated reading (mmHg)
-0.01112	Male	LV	1.63E-02	Hand grip strength (right)
-0.01095	Female	LV	8.07E-02	Hand grip strength (right)
-0.01008	Female	MYO	8.36E-01	Oily fish intake
-0.01006	Female	LA	5.31E-01	Townsend score
-0.00996	Female	LV	5.78E-01	Education level
-0.00976	Male	RA	4.08E-01	Glycated haemoglobin (HbA1c)
-0.00938	Male	LA	1.07E-03	Alanine aminotransferase
-0.00935	Male	RA	4.38E-02	Hand grip strength (left)
-0.00922	Female	LA	3.30E-01	Glycated haemoglobin (HbA1c)
-0.00864	Female	RV	2.36E-01	Glycated haemoglobin (HbA1c)
-0.00798	Male	RV	8.73E-02	Hand grip strength (left)
-0.00797	Male	LA	6.64E-01	Liver PDFF (proton density fat fraction)

-0.00778	Female	LA	8.37E-01	Beef intake
-0.00764	Male	MYO	1.20E-04	Systolic blood pressure, automated reading (mmHg)
-0.00706	Male	RA	4.92E-01	Time spent watching television
-0.00659	Male	RV	9.75E-01	Cholesterol
-0.00619	Male	RV	1.91E-01	Hand grip strength (right)
-0.00618	Male	RA	1.76E-01	Hand grip strength (right)
-0.0061	Male	RA	9.31E-01	Mouth/teeth dental problems
-0.00603	Female	RA	9.15E-01	Smoking status
-0.0058	Male	RV	7.53E-01	Pulse wave Arterial Stiffness index (m/s)
-0.00558	Male	LA	2.00E-01	Diastolic blood pressure, automated reading (mmHg)
-0.00541	Female	LA	9.66E-01	Abdominal subcutaneous adipose tissue volume
-0.00486	Male	LA	7.52E-01	Number of days/week of moderate physical activity 10+ minutes
-0.00475	Female	LA	1.99E-01	Alanine aminotransferase
-0.00418	Male	RV	6.83E-01	Glycated haemoglobin (HbA1c)
-0.00408	Male	LV	6.67E-02	Systolic blood pressure, automated reading (mmHg)
-0.00401	Female	LA	2.64E-01	Pulse rate
-0.00371	Male	MYO	7.01E-01	Glycated haemoglobin (HbA1c)
-0.00358	Male	LA	8.49E-01	Neuroticism score
-0.00352	Female	RA	6.52E-01	Hand grip strength (left)
-0.00341	Female	LV	9.05E-01	Body mass index
-0.00339	Female	RA	7.75E-01	Glycated haemoglobin (HbA1c)
-0.00316	Female	LA	1.62E-01	Systolic blood pressure, automated reading (mmHg)
-0.00231	Female	RA	7.42E-01	Hand grip strength (right)
-0.00186	Female	RA	9.64E-01	Number of vehicles in household
-0.00175	Female	RA	8.78E-01	Neuroticism score
-0.00081	Female	LV	8.07E-02	Peak expiratory flow (PEF)
-0.0008	Male	RA	7.40E-01	Alanine aminotransferase
-0.00072	Male	LA	4.58E-01	Gamma glutamyltransferase
-0.00059	Male	RA	7.72E-01	Systolic blood pressure, automated reading (mmHg)
-0.00047	Female	RV	9.85E-01	Body mass index
-0.00046	Male	RV	8.82E-01	Oestradiol
-0.0003	Female	RV	5.25E-01	Peak expiratory flow (PEF)
-0.00027	Female	MYO	6.35E-01	Peak expiratory flow (PEF)
-0.00015	Female	RV	9.91E-01	Number of treatments/medications taken
-0.00013	Female	LA	8.19E-01	Peak expiratory flow (PEF)
-9.15E-05	Male	RV	9.98E-01	LDL direct
-6.88E-05	Female	MYO	6.04E-01	Oestradiol
-4.08E-05	Female	RA	8.80E-01	Oestradiol
-3.48E-05	Male	RV	8.93E-01	Peak expiratory flow (PEF)
-3.27E-06	Female	LV	9.85E-01	Oestradiol
2.17E-05	Female	LA	8.69E-01	Oestradiol
2.76E-05	Female	RV	8.20E-01	Oestradiol
0.000118	Female	LV	9.24E-01	Gamma glutamyltransferase
0.000323	Female	LA	9.51E-01	Hand grip strength (right)
0.000354	Male	LV	2.69E-01	Peak expiratory flow (PEF)
0.000406	Female	LA	9.66E-01	Waist circumference

0.000409	Male	MYO	1.83E-01	Peak expiratory flow (PEF)
0.000425	Female	LA	7.49E-01	Gamma glutamyltransferase
0.000732	Female	RA	1.88E-01	Peak expiratory flow (PEF)
0.000859	Female	MYO	9.46E-01	Townsend score
0.000874	Male	LA	1.15E-02	Peak expiratory flow (PEF)
0.000923	Male	RA	9.76E-03	Peak expiratory flow (PEF)
0.000964	Female	RA	6.40E-01	Gamma glutamyltransferase
0.001009	Male	RV	7.53E-01	Systolic blood pressure, automated reading (mmHg)
0.001025	Male	RA	9.29E-01	Neuroticism score
0.001036	Male	RA	4.08E-01	Gamma glutamyltransferase
0.00104	Male	RV	9.74E-01	Body mass index
0.00114	Female	MYO	9.46E-01	Fluid intelligence score
0.001144	Male	MYO	5.07E-01	Oestradiol
0.001147	Male	RV	3.37E-01	Gamma glutamyltransferase
0.001317	Male	LV	8.41E-01	Glycated haemoglobin (HbA1c)
0.001333	Male	LV	3.87E-01	Gamma glutamyltransferase
0.001419	Female	LV	9.72E-01	Beef_intake
0.001551	Male	MYO	1.48E-01	Gamma glutamyltransferase
0.00162	Female	LA	9.68E-01	Number of vehicles in household
0.00212	Male	LA	6.70E-01	Hand grip strength (right)
0.002178	Male	LV	6.62E-01	Alanine aminotransferase
0.002202	Male	RA	9.54E-01	Trunk fat mass
0.002232	Male	LV	8.92E-01	Fluid intelligence score
0.002275	Female	LV	9.24E-01	Glycated haemoglobin (HbA1c)
0.002476	Male	LV	3.27E-01	Oestradiol
0.002503	Female	RV	2.76E-02	Gamma glutamyltransferase
0.002796	Female	LA	7.54E-01	Hand grip strength (left)
0.003098	Male	RV	3.37E-01	Alanine aminotransferase
0.003178	Female	LV	5.08E-01	Alanine aminotransferase
0.003229	Female	MYO	7.22E-03	Gamma glutamyltransferase
0.0036	Male	LA	7.93E-02	Oestradiol
0.003685	Female	RV	9.23E-01	Number of vehicles in household
0.003753	Male	RA	8.19E-02	Oestradiol
0.003826	Male	LA	2.11E-01	Pulse rate
0.003916	Male	RA	9.40E-01	Whole body fat mass
0.004289	Male	RV	8.82E-01	Testosterone
0.004591	Female	RA	2.03E-01	Pulse rate
0.004768	Male	RA	7.10E-01	Townsend score
0.005053	Male	MYO	9.06E-01	LDL direct
0.00509	Female	RA	9.15E-01	Oily fish intake
0.005167	Male	RA	8.51E-01	Waist circumference
0.006194	Female	RV	2.76E-02	Alanine aminotransferase
0.006251	Female	RA	8.59E-01	Cholesterol
0.006333	Female	RV	7.60E-01	Fluid intelligence score
0.006958	Female	RA	8.60E-01	Education level
0.007081	Male	MYO	4.98E-03	Alanine aminotransferase

0.007166	Female	LA	9.76E-02	Diastolic blood pressure, automated reading (mmHg)
0.007544	Male	LA	8.49E-01	Financial situation satisfaction
0.008225	Female	RA	3.35E-02	Alanine aminotransferase
0.008231	Male	LA	1.12E-01	Hand grip strength (left)
0.008304	Female	RA	1.45E-05	Systolic blood pressure, automated reading (mmHg)
0.008628	Female	LV	9.24E-01	Cholesterol
0.008963	Female	RV	1.57E-07	Systolic blood pressure, automated reading (mmHg)
0.009011	Female	MYO	3.00E-03	Alanine aminotransferase
0.010129	Female	RA	5.89E-01	Pulse wave Arterial Stiffness index (m/s)
0.010259	Female	LV	1.04E-07	Systolic blood pressure, automated reading (mmHg)
0.01159	Female	MYO	8.36E-01	Smoking status
0.011616	Female	LV	5.57E-01	Fluid intelligence score
0.012859	Male	LA	8.59E-01	Mouth/teeth dental problems
0.013018	Female	LV	4.80E-01	Number of treatments/medications taken
0.013066	Female	RV	2.51E-01	Neuroticism score
0.013227	Female	LV	3.14E-01	Neuroticism score
0.013374	Female	LA	8.94E-01	Trunk fat mass
0.013573	Male	RV	4.96E-01	Number of treatments/medications taken
0.013734	Female	MYO	9.30E-01	Mouth/teeth dental problems
0.013779	Male	MYO	3.32E-05	Diastolic blood pressure, automated reading (mmHg)
0.013796	Female	MYO	3.84E-14	Systolic blood pressure, automated reading (mmHg)
0.013914	Male	LA	4.30E-01	Waist circumference
0.014259	Male	MYO	7.62E-01	Pork intake
0.014809	Female	LV	2.77E-01	Time spent watching television
0.015045	Female	MYO	6.11E-02	Glycated haemoglobin (HbA1c)
0.015446	Female	RV	7.43E-01	Average total household income before tax
0.015643	Female	LA	7.49E-01	Triglycerides Level
0.016005	Male	MYO	2.21E-01	Townsend score
0.016016	Male	RA	2.46E-07	Pulse rate
0.016899	Male	RA	8.51E-01	Total lean tissue volume
0.017276	Male	RV	5.33E-08	Diastolic blood pressure, automated reading (mmHg)
0.017366	Female	LA	2.39E-01	Neuroticism score
0.017673	Female	MYO	9.40E-02	Time spent watching television
0.017893	Male	RA	4.94E-01	Pulse wave Arterial Stiffness index (m/s)
0.017952	Female	RV	1.80E-09	Pulse rate
0.018164	Male	MYO	1.21E-01	Neuroticism score
0.018332	Female	LV	5.78E-01	Average total household income before tax
0.01842	Male	LV	7.14E-01	Pork intake
0.018513	Female	RA	3.39E-01	Liver PDFF (proton density fat fraction)
0.018655	Female	LA	4.71E-01	Whole body fat mass
0.018734	Female	MYO	5.49E-01	Body mass index
0.019297	Male	RV	8.25E-01	Forced expiratory volume in 1-second (FEV1), Best measure
0.02002	Male	LV	3.25E-01	Education level
0.020101	Male	LA	2.56E-01	Education level
0.020173	Female	RV	3.81E-11	Diastolic blood pressure, automated reading (mmHg)
0.020384	Male	RA	4.00E-01	Education level

0.02047	Female	LA	3.76E-01	Education level
0.020695	Male	RV	6.49E-01	Pork intake
0.02131	Male	RV	1.31E-13	Pulse rate
0.021573	Female	RV	7.69E-02	Time spent watching television
0.021827	Male	LV	2.69E-01	Number of treatments/medications taken
0.022173	Male	LV	1.68E-10	Diastolic blood pressure, automated reading (mmHg)
0.022195	Female	LA	2.36E-01	Number of treatments/medications taken
0.022448	Female	MYO	6.07E-01	Total lean tissue volume
0.02258	Male	RA	6.87E-11	Diastolic blood pressure, automated reading (mmHg)
0.022957	Female	RA	1.88E-01	Number of treatments/medications taken
0.023372	Male	RA	8.51E-01	Total trunk fat volume
0.023783	Male	LA	6.64E-01	Total lean tissue volume
0.024256	Male	RV	1.78E-01	Liver PDFF (proton density fat fraction)
0.02427	Male	LV	6.07E-02	Time spent watching television
0.024882	Female	MYO	5.11E-02	Neuroticism score
0.025958	Female	MYO	2.62E-16	Pulse rate
0.025995	Male	LA	7.74E-02	Townsend score
0.02676	Male	MYO	2.33E-02	Waist circumference
0.02712	Female	LA	6.78E-01	Pork intake
0.028351	Male	RV	7.11E-02	Townsend score
0.028363	Male	RV	1.04E-02	Neuroticism score
0.028678	Male	MYO	5.77E-01	Beef intake
0.028733	Female	RV	2.35E-03	Waist circumference
0.029013	Female	LA	6.47E-01	Total trunk fat volume
0.029054	Male	MYO	1.64E-23	Pulse rate
0.029402	Male	LA	1.24E-01	Fluid intelligence score
0.029977	Female	RA	8.01E-01	Fed-up feelings
0.030005	Male	LV	3.88E-01	Body mass index
0.030019	Male	MYO	1.14E-01	Pulse wave Arterial Stiffness index (m/s)
0.030209	Male	RV	4.61E-03	Time spent watching television
0.030333	Female	RA	4.26E-20	Diastolic blood pressure, automated reading (mmHg)
0.030973	Male	LV	5.79E-02	Townsend score
0.031016	Male	LV	1.70E-02	Neuroticism score
0.032119	Female	LA	2.04E-01	Liver PDFF (proton density fat fraction)
0.032471	Female	LV	1.81E-22	Pulse rate
0.032482	Female	LV	6.96E-01	Smoking status
0.03291	Female	LV	1.81E-22	Diastolic blood pressure, automated reading (mmHg)
0.033713	Male	RV	3.38E-03	Waist circumference
0.03381	Female	RA	1.34E-03	Waist circumference
0.034311	Female	RA	6.40E-01	LDL direct
0.034434	Male	LA	6.58E-01	Pork intake
0.034603	Female	RA	4.63E-01	Average total household income before tax
0.03513	Female	LV	1.05E-03	Waist circumference
0.035547	Female	MYO	1.32E-28	Diastolic blood pressure, automated reading (mmHg)
0.03557	Male	LV	4.92E-01	Beef intake
0.036067	Male	LV	2.63E-31	Pulse rate

0.037388	Female	RV	1.54E-02	Whole body fat mass
0.037587	Female	RV	2.84E-02	Pulse wave Arterial Stiffness index (m/s)
0.03759	Male	RA	4.38E-02	Fluid intelligence score
0.038001	Female	LV	4.97E-02	Pulse wave Arterial Stiffness index (m/s)
0.03804	Female	LA	8.69E-01	Testosterone
0.038597	Male	LV	1.67E-03	Waist circumference
0.038675	Female	MYO	3.56E-02	Pulse wave Arterial Stiffness index (m/s)
0.03923	Male	RA	4.23E-01	Beef intake
0.040347	Male	MYO	2.87E-02	Whole body fat mass
0.040519	Female	RV	8.20E-01	Testosterone
0.040767	Female	RA	8.31E-02	Fluid intelligence score
0.041228	Female	LV	5.57E-01	Mouth/teeth dental problems
0.042962	Female	MYO	4.47E-03	Number of treatments/medications taken
0.04317	Male	RV	1.94E-02	Whole body fat mass
0.044335	Female	RV	3.95E-01	Smoking status
0.044336	Male	MYO	2.81E-01	Testosterone
0.044729	Male	MYO	1.95E-05	Time spent watching television
0.044991	Female	RV	1.14E-02	Liver PDFF (proton density fat fraction)
0.045188	Female	RA	3.65E-01	Abdominal subcutaneous adipose tissue volume
0.045695	Female	LV	1.03E-02	Whole body fat mass
0.047249	Female	LA	7.54E-01	Forced expiratory volume in 1-second (FEV1), Best measure
0.047391	Female	LV	1.71E-02	Liver PDFF (proton density fat fraction)
0.04784	Female	RV	4.49E-01	Ever unenthusiastic/disinterested for a whole week
0.048272	Male	LA	4.20E-01	Oily fish intake
0.049317	Female	MYO	1.58E-01	Cholesterol
0.050001	Male	RA	4.23E-01	Pork intake
0.050022	Female	LA	1.33E-02	Fluid intelligence score
0.050123	Male	RA	2.87E-01	Forced vital capacity (FVC)
0.05041	Female	RA	1.94E-01	Trunk fat mass
0.050594	Female	RV	1.38E-01	Cholesterol
0.050966	Male	RA	1.51E-02	Number of treatments/medications taken
0.051335	Female	LA	2.50E-01	Average total household income before tax
0.051703	Male	LV	6.29E-03	Liver PDFF (proton density fat fraction)
0.051759	Female	MYO	2.10E-07	Waist circumference
0.051997	Male	RA	3.34E-01	Average total household income before tax
0.055749	Male	MYO	4.24E-01	Smoking status
0.057337	Female	MYO	4.63E-04	Whole body fat mass
0.057784	Male	MYO	9.18E-04	Number of treatments/medications taken
0.0595	Female	RA	1.06E-03	Whole body fat mass
0.060208	Male	RA	7.64E-01	Fed-up feelings
0.061018	Male	RV	1.91E-01	Forced vital capacity (FVC)
0.06288	Male	LA	7.93E-02	Testosterone
0.063131	Male	RA	8.19E-02	Testosterone
0.065033	Male	RA	2.97E-01	Oily fish intake
0.066165	Male	MYO	3.72E-04	Liver PDFF (proton density fat fraction)
0.066824	Female	RA	2.58E-02	Body mass index

0.067624	Female	RA	3.27E-01	Beef intake
0.068038	Female	RA	3.27E-01	Pork intake
0.069743	Male	LV	2.11E-01	Triglycerides Level
0.071108	Female	LA	4.05E-01	Smoking status
0.073117	Female	MYO	8.24E-05	Liver PDFF (proton density fat fraction)
0.0748	Male	RV	9.63E-02	Triglycerides Level
0.076552	Female	LV	2.46E-01	LDL direct
0.078694	Female	MYO	7.75E-02	Beef intake
0.078778	Female	RV	7.69E-02	Beef intake
0.080425	Female	LA	3.61E-01	Fed-up feelings
0.08075	Male	LV	3.11E-02	Testosterone
0.082287	Female	RV	2.51E-01	Fed-up feelings
0.08569	Female	RA	3.29E-02	Total trunk fat volume
0.085981	Male	LA	3.81E-01	Visceral adipose tissue volume
0.086189	Female	RV	7.69E-02	Pork intake
0.086298	Male	LA	4.20E-01	Smoking status
0.090747	Female	LA	2.89E-01	Mouth/teeth dental problems
0.091294	Male	LA	4.60E-01	Ever unenthusiastic/disinterested for a whole week
0.091561	Male	LV	5.23E-06	Whole body fat mass
0.095059	Female	RV	1.80E-01	Mouth/teeth dental problems
0.09871	Female	MYO	1.79E-01	Fed-up feelings
0.099598	Female	LA	2.36E-01	Forced vital capacity (FVC)
0.100327	Female	RV	2.51E-01	Nervous feelings
0.108701	Female	LA	1.09E-01	Total lean tissue volume
0.114163	Female	RV	1.47E-02	LDL direct
0.114343	Male	RA	3.71E-01	Visceral adipose tissue volume
0.115573	Male	LV	2.05E-01	Nervous feelings
0.116879	Female	MYO	7.75E-02	Pork intake
0.120035	Female	LV	1.44E-01	Fed-up feelings
0.122298	Female	RA	4.65E-02	Triglycerides Level
0.122706	Male	LA	1.12E-01	Forced expiratory volume in 1-second (FEV1), Best measure
0.124078	Male	LV	1.67E-03	Trunk fat mass
0.127514	Male	RA	7.19E-02	Forced expiratory volume in 1-second (FEV1), Best measure
0.128558	Male	LV	1.13E-01	Ever unenthusiastic/disinterested for a whole week
0.12921	Male	RV	6.33E-02	Ever unenthusiastic/disinterested for a whole week
0.132066	Male	MYO	1.22E-01	Nervous feelings
0.133002	Male	MYO	8.46E-02	Mouth/teeth dental problems
0.140762	Female	MYO	1.05E-01	Nervous feelings
0.141867	Male	RV	8.73E-02	Mouth/teeth dental problems
0.142461	Male	RA	4.08E-01	HDL cholesterol
0.144279	Female	RA	1.88E-01	Forced expiratory volume in 1-second (FEV1), Best measure
0.145804	Female	LA	2.04E-01	Visceral adipose tissue volume
0.146015	Male	LA	3.14E-01	HDL cholesterol
0.153246	Female	MYO	1.59E-03	LDL direct
0.154065	Female	MYO	1.87E-05	Trunk fat mass
0.164722	Female	LA	4.52E-02	Ever unenthusiastic/disinterested for a whole week

0.165059	Male	MYO	1.86E-05	Trunk fat mass
0.165441	Female	LV	2.17E-05	Trunk fat mass
0.166173	Male	RV	8.94E-06	Trunk fat mass
0.170246	Male	MYO	5.88E-03	Abdominal subcutaneous adipose tissue volume
0.175765	Female	LV	7.50E-02	Nervous feelings
0.176136	Female	MYO	4.63E-04	Abdominal subcutaneous adipose tissue volume
0.179568	Female	RA	3.91E-04	Total lean tissue volume
0.188082	Female	RV	1.50E-08	Trunk fat mass
0.190211	Male	LV	1.71E-02	Mouth/teeth dental problems
0.190316	Male	RV	1.57E-03	Abdominal subcutaneous adipose tissue volume
0.194299	Male	MYO	9.93E-03	Fed-up feelings
0.200027	Male	LV	1.70E-02	Fed-up feelings
0.204291	Male	MYO	1.31E-08	Triglycerides Level
0.210139	Male	RV	1.62E-07	Total trunk fat volume
0.213111	Female	MYO	6.38E-02	Testosterone
0.21504	Male	LV	1.12E-03	Abdominal subcutaneous adipose tissue volume
0.221961	Male	LA	1.81E-06	Forced vital capacity (FVC)
0.222448	Female	LV	4.44E-05	Abdominal subcutaneous adipose tissue volume
0.233626	Male	RV	9.34E-03	Nervous feelings
0.233738	Female	RV	7.56E-07	Abdominal subcutaneous adipose tissue volume
0.246222	Male	RV	7.91E-04	Fed-up feelings
0.253944	Male	RV	5.86E-06	Visceral adipose tissue volume
0.256255	Female	RV	3.21E-13	Total trunk fat volume
0.258549	Male	MYO	1.04E-03	Ever unenthusiastic/disinterested for a whole week
0.26172	Male	LV	9.68E-10	Total trunk fat volume
0.26459	Female	RV	3.30E-08	Triglycerides Level
0.273218	Female	RA	1.34E-03	Visceral adipose tissue volume
0.276088	Female	LV	6.48E-12	Total trunk fat volume
0.285929	Female	MYO	4.05E-14	Total trunk fat volume
0.32992	Male	LV	2.92E-08	Visceral adipose tissue volume
0.347695	Female	LV	5.85E-11	Triglycerides Level
0.347953	Male	MYO	2.65E-19	Total trunk fat volume
0.462521	Female	MYO	7.71E-21	Triglycerides Level
0.53184	Male	MYO	5.39E-23	Visceral adipose tissue volume
0.564127	Female	RV	8.34E-14	Visceral adipose tissue volume
0.691806	Female	LV	9.78E-16	Visceral adipose tissue volume
0.846548	Female	MYO	1.69E-26	Visceral adipose tissue volume

**Supplementary Table 4 footnote.** HDL: high-density lipoprotein; LA: left atrium; LDL: low-density lipoprotein; LV: left ventricle; MYO: myocardium; RA: right atrium; RV: right ventricle.